HHS Public Access

Author manuscript

Mater Sci Eng C Mater Biol Appl. Author manuscript; available in PMC 2022 January 01.

Published in final edited form as:

Mater Sci Eng C Mater Biol Appl. 2021 January ; 120: 111748. doi:10.1016/j.msec.2020.111748.

Osteogenic Differentiation Cues of the Bone Morphogenetic Protein-9 (BMP-9) and Its Recent Advances in Bone Tissue Regeneration

Angshuman Bharadwaz[a], **Ambalangodage C. Jayasuriya**[a,b,*]

[a]Biomedical Engineering Program, Department of Bioengineering, College of Engineering, The University of Toledo, Toledo OH, USA

[b]Department of Orthopaedic Surgery, College of Medicine and Life Sciences, The University of Toledo, Toledo OH, USA

Abstract

Bone regeneration using bioactive molecules and biocompatible materials is growing steadily with the advent of the new findings in cellular signaling. Bone Morphogenetic Protein (BMP)-9 is a considerably recent discovery from the BMP family that delivers numerous benefits in osteogenesis. The Smad cellular signaling pathway triggered by BMPs is often inhibited by Noggin. However, BMP-9 is resistant to Noggin, thus, facilitating a more robust cellular differentiation of osteoprogenitor cells into preosteoblasts and osteoblasts. This review encompasses a general understanding of the Smad signaling pathway activated by the BMP-9 ligand molecule with its specific receptors. The robust osteogenic cellular differentiation cue provided by BMP-9 has been reviewed from a bone regeneration perspective with several *in vitro* as well as *in vivo* studies reporting promising results for future research. The effect of the biomaterial, chosen in such studies as the scaffold or carrier matrix, on the activity of BMP-9 and subsequent bone regeneration has been highlighted in this review. The non-viral delivery technique for BMP-9 induced bone regeneration is a safer alternative to its viral counterpart. The recent advances in non-viral BMP-9 delivery have also highlighted the efficacy of the protein molecule at a low dosage. This opens a new horizon as a more efficient and safer alternative to BMP-2, which was prevalent among clinical trials; however, BMP-2 applications have reported its downsides during bone defect healing such as cystic bone formation.

Graphical Abstract

[*]Corresponding Author Department of Orthopaedic Surgery, University of Toledo Medical Center, 3000 Arlington Avenue, Toledo, OH 43614, USA, Tel: +1-419-383-6557, Fax: +1-419-383-3526, a.jayasuriya@utoledo.edu.

Conflict of interest: none

Declaration of competing interest

The authors declare that they have no known competing financial interests or personal relationships that could have appeared to influence the work reported in this paper.

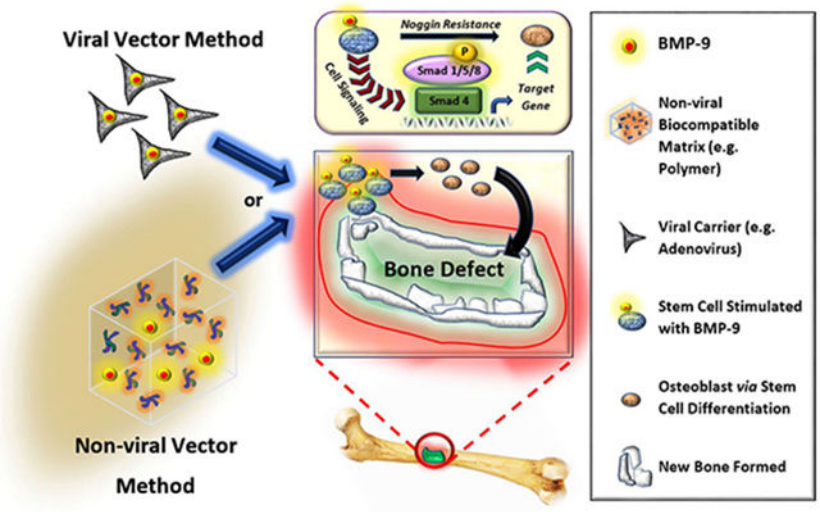

Keywords

Bone morphogenetic protein (BMP); bone regeneration; scaffold; Smad; cell signaling; non-viral delivery

1. Introduction

One of the key tissue systems inside our body, the skeletal system, is crafted synchronously from bones. The bones inside our body comprise of a major portion as minerals and the remaining component of non-mineral organic matrix. The bone performs a myriad of critical functions inside the body that range from providing the body with the needed structural integrity, facilitation of locomotor abilities, protection of vital organs, an integument for bone marrow that facilitates blood cell synthesis, and as a sump for storing essential minerals such as phosphorous and calcium in the body [1-5]. Five primary kinds of cells formulate the bone tissue: pre-osteoblasts, osteoblasts, osteoclasts, osteocytes, and bone-lining cells. A constant phenomenon of bone absorption and redeposition, known as remodeling, occurs within the body that is facilitated by these cells as a response to new stress. The remodeling process is triggered with the resorption of the existing bone by osteoclasts, followed by new bone deposition by osteoblasts; there is a brief reversible transition phase between the resorption and redeposition. The osteocytes play a crucial role in facilitating this remodeling process with their mechano-transduction property. The bone-lining cells cover the existing bone that needs to be excluded in that current remodeling trigger. [6-12].

The remodeling of bone is a constant process, however, critical-sized bone defects caused usually by trauma are difficult to heal by the natural body processes and require the use of auxiliary bone regeneration techniques. Functional bone grafting has seen a spike in its demand across the globe due to the increasing cases of bone disorders. About 15 million patients with bone-related disorders spend approximately $45 billion annually worldwide. The United States alone sees an approximate expenditure of $2.5 billion from around 1.6

million patients annually. These patients include osteoporotic defects of the bone as well as trauma-related fractures [13-15]. Autografting, which uses the bone tissue harvested from the patient, is a common technique for the treatment of bone defects. The induction of osteogenesis by the cells already present within the autograft facilitates the formation of new bone in the defect site. Such a technique facilitates bone formation as it provides a porous three-dimensional scaffold structure that promotes angiogenesis as well as differentiation of stem cells. Allografting is another technique that utilizes extracted bone tissue from a donor or cadaver. Allografting also provides essential cues such as bone morphogenetic proteins (BMPs) that facilitate the differentiation of stem cells to osteoprogenitor cells [16]. However, several limitations such as immunogenicity, inadequate blood supply, pain, infection, donor site morbidity, scarring, bleeding, and inadequate supply of grafts, etc. pose a hindrance to autografting and allografting methods [17-26].

In order to overcome the limitations posed by the current standard practices of bone healing, the use of BMPs is regarded as a favorable method for aiding in the regeneration process of bone in critical-sized bone defects. BMPs hail from the transforming growth factor-beta (TGF-β) superfamily and play a critical role in the formation of osteoprogenitor cells from mesenchymal stem cells (MSCs). In the later 20^{th} century BMPs were first discovered serendipitously by an orthopaedic surgeon, Dr. Marshall Urist, as BMPs were found to have induced bone formation in muscle tissue [27-33]. Apart from osteogenesis, BMPs also aid in several other processes such as hepatocyte proliferation, adipogenesis, angiogenesis etc. [34-37]. In Bone Tissue Engineering (BTE), adequate bone defect healing relies on the interaction of the progenitor cells with their respective differentiation cues, viz. BMPs that are optimally delivered via the use of specifically chosen biomaterial-based scaffold/delivery systems [38-42]. Several members from the BMP family, such as BMP-2, BMP-7, and BMP-9, have delivered promising results during bone healing, however, only BMP-9 amongst them possesses the property to resist inhibition of the Smad cellular signaling pathway induced by Noggin [43-52]. Thus, out of the fourteen (14) BMPs known, BMP-9 was reported as one of the few BMPs as very promising for the derivation of osteoprogenitor cells from stem cells through differentiation [53]. Several *in vitro* and *in vivo* studies using BMP-9 have proved its efficacy towards osteogenesis, as well as its resistance to Noggin [54-57]. BMP-9 induces osteogenesis through a series of signaling pathway cascades that mediate crosstalk with other intrinsic signaling pathways such as hairy/enhancer-of-split related with YRPW motif protein 1 (Hey1), cysteine rich with epidermal growth factor (EGF) like domain 2 (Creld2), Janus kinase (JAK)-signal transducer and activator of transcription (STAT) pathway, insulin-like growth factor 1 (IGF-1), protein kinase A (PKA)/ cyclic adenosine monophosphate - response element binding protein (CREB) signaling, etc. [57-63]. This review is drafted around the use of BMP-9 for its property of osteogenic induction, cell differentiation, and subsequent bone formation. A case by case basis of review as it pertains to bone regeneration and the use of BMP-9, in both non-viral and viral vector-based delivery systems has been discussed, along with the effect of the biomaterial on the osteogenic differentiation of stem cells, if any, and the overall bone regeneration process. The choice of the biomaterial is a quintessential parameter in facilitating adequate bone defect healing, and hence this review tries to highlight the intrinsic effect of the biomaterial in synergy with BMP-9. This review also encompasses the general interaction and signaling

mechanism of BMP-9 in the osteogenesis signaling pathways. The current literature has a limited number of resources incorporating the consolidated review of various recent studies related to BMP-9 and its role in regenerative medicine. A review article dedicated solely to the application of BMP-9 in recent times for bone tissue regeneration would be beneficial, especially with an added focus on the biomaterial used for incorporating BMP-9. Therefore, this review has been designed primarily to address the impact of BMP-9 mediated osteogenic differentiation and subsequent bone regeneration on the specific field of bone tissue regeneration.

2. Cellular Signaling and Interaction of BMP-9

2.1. Mechanism of Smad Pathway and Resistance to Noggin

BMP-9 communicates within the cellular signaling mechanism through certain specific as well as non-specific cellular signaling pathways. The activation of the intracellular mediator Smad is the key target of the BMP-9 signaling cascade. The signaling cascade for BMP-9 gets triggered when the BMP ligand binds with the heterodimer of type I and type II BMP receptor (BMPR). The binding of the ligand to its receptor triggers the phosphorylation of Smad 1 or its homologues Smad 5 or Smad 8 within the cytoplasm that further forms a heterodimer with cytoplasmic Smad 4 and translocate to the nucleus to activate the target genes, as shown in Figure 1 (I) [37, 64-66]. The Smad 4 complex with Smad 1/5/8 is a key component of this signaling cascade that facilitates the nuclear translocation of the Smad complex, which is evident from Figure 1 (II); the study incorporated recombinant adenoviruses expressing siRNA targeted Smad 4 (si-Smad 4) as Smad 4 knockdown, with adenoviruses expressing only green fluorescence protein or red fluorescence protein as a negative control (NC), and uninfected cells as Blank. During this process of triggering the Smad signaling pathway, type I TGF-β receptors, such as anaplastic lymphoma kinase (ALK) 1 and ALK 2, facilitate Smad activation along with BMP; whereas dominant negative type II TGF-β receptors, such as dominant negative BMP receptor type II (DN-BMPRII), dominant negative activin receptor type II (DN-ActRII), and dominant negative activin receptor type IIB (DN-ActRIIB), have been reported to be inhibitors of the Smad activation sequence, thus downregulating the activity of BMP; thereby exhibiting the significant functionality of both types of receptors in the osteogenic differentiation of stem cells using BMP-9. Moreover, the mitogen activated protein kinase (MAPK) p38 has a significant influence over the phosphorylation of Smad, which in turn upregulates the BMP activity. However, this sequence of Smad phosphorylation is downregulated or inhibited by extracellular signal-regulated kinases (ERK) 1/2 [67-73].

A known antagonist of BMPs, Noggin, is a glycoprotein that was initially identified as a part of the Spermann organizer and induces the formation of neural tissue; Noggin has a molecular mass of around 64 kDa [74-77]. The mechanism of inhibition of the BMP signaling pathway by Noggin is reported to occur by binding to the ligand domains in type I and II BMPR, thereby blocking all binding sites for incoming BMP ligands [78]. However, studies have shown that Noggin does not affect the osteogenic function of BMP-9, unlike some other BMPs such as BMP 2/4/5/6/7 [75, 79]. It has been reported that BMP-9 stimulated cell lines had shown a high ALP activity as compared to BMP 2/4/6/7 stimulated

cells [45]. The advantages of BMP-9 over BMP-2 as evident from notable studies have been summarized in Table 1. As shown in Figure 2 (IA – d), the nuclear translocation of Smad 1/5/8 was facilitated in the presence of BMP-9 in comparison BMP-2; thus, displaying resistance of BMP-9 to the inhibitory action triggered by Noggin in comparison to BMP 2 Figure 2 (IA – b). The resistance of BMP-9 to Noggin inhibition was also reported for the expression of Smad 6 and Smad 7, as shown in Figure 2 (IB). Moreover, BMP-9 stimulated muscle precursor cell line C2C12 or Mouse Embryonic Fibroblasts (MEF) displayed formation of larger ectopic bone, as compared to BMP 2/4/6/7 that showed smaller or negligible ectopic bone formation, as shown in Figure 2 (IIA); this also highlights the significant inhibitory function of Noggin on the other BMPs except BMP-9. Hematoxylin and Eosin (H&E) staining results showed that BMP-9 was able to induce the bone formation in both cell lines, C2C12 - Figure 2 (IIB) and MEFs - Figure 2 (IIC), in the absence and presence of Noggin as shown in Figure 2 (II – a vs. d). However, a noticeable reduction in the bone matrix was assessed through trichrome staining for bone formation with the presence of Noggin Figure 2 (IIC – a vs. d). Further, immunohistochemical staining using antibodies against osteopontin (OPN) and osteocalcin (OCN) proved that those late osteogenic markers were also resistant towards the inhibitory effect of Noggin [45].

2.2. Mediators that Influence BMP-9 Induced Osteogenesis

One of the key transcription factors activated by the BMP-9/SMAD signaling pathway is runt-related (RUNX2). RUNX2 is widely known for its quintessential functionality during bone formation from several studies [83-87]. The RUNX proteins have denoted the crosstalk of microRNAs (miRNAs) during osteogenesis. miRNAs are RNAs, approximately 22 nucleotides long, that are not involved in coding and their function is to act as down-regulators of post-transcriptional activity by the degradation of target mRNA; this has been assessed as a key event in the bone formation process [88]. Another study using bone marrow MSCs (BMMSCs) and miRNA-21 displayed enhanced osteogenic differentiation of the BMMSCs with miRNA-21 upregulation [89]. Whereas, miRNA-21 knockout samples showed reduced osteogenesis of the BMMSCs; this proved the significant effect that miRNA-21 has on the osteogenic differentiation pathway. Smad 7, which is known for its inhibitory effect on the BMP signaling pathway by regulating the intensity of the phosphorylated SMAD 1/5/8/ signaling cascade, is reported to be a target for the miRNA-21 [89, 90]. miRNA-21 inhibits the translation of Smad 7 by targeting the 3’-UTR of Smad 7 mRNA. Knocking down of miRNA-21 expressed an increase in Smad 7 which further influences phosphorylation of Smad 1/5/8. Excessive Smad 7 reduces RUNX2 expression which results in poor osteogenic differentiation of the stem cells and therefore lower bone growth. These results have been confirmed using histology of regenerated bone as shown in Figure 3 in an *in vivo* experiment comparing wild-type mice with MiR-21 knockouts [89]. Also, other studies have reported that a few other members of the RUNX family, namely RUNX1 and RUNX3 are also key players in the BMP-9 induced osteogenic differentiation of stem cells [91, 92].

Inhibitors of differentiation (Ids) helix-loop-helix (HLH) factors are another set of proteins that are expressed ubiquitously and are affected by BMP-9 induced osteogenic signaling. Ids were initially discovered as inhibitors of basic HLH (bHLH) transcription factors coupling

with muscle-specific gene expressions. The cytosine (C), adenine (A), nucleotide (N), guanine (G), and thymine (T) containing CANNTG promoter element region is the target for the transcription of genes by bHLH dimerization. As inhibitors, Ids bind with the bHLH which in turn prevents the DNA binding and subsequent gene transcription [93-101]. It is known that Id genes 1/2/3 are upregulated by BMP-9 stimulated stem cells. It was also found that the knockdown of Id genes had a significant effect on the osteogenic differentiation induced by BMP-9. These Ids are expressed at the onset of cell stimulation by BMPs only rather than at the terminal phase of the cell differentiation process. Overexpression of these Ids has been reported as a cause for reduced formation of osteoblasts and enhanced proliferation rate of cells. These Id genes have been also reported to be dependent on the Smad 4 signaling pathway [55, 102].

The Hairy/Enhancer of split-related proteins (HERP) belongs to the family of bHLH proteins that are part of the BMP-9 signaling pathway. The Notch signaling pathway that decides the fate of a cell also directly triggers HERP and the primary function of HERP is to act as a repressor of transcriptional activity [32, 103-105]. Hey2 protein, from the HERP family, shows a spatio-temporal pattern for expression and has been discovered during the embryonic development stages of the craniofacial area, the heart, somite, and the nervous system [106, 107]. A study on pluripotent MSCs using BMP-9 induced cell differentiation methodology showed a significant upregulation of Hey1 expression at the onset of the cell differentiation process in MSCs [57]. Hey1 was also reported in the same study as the direct target of the Smad signaling pathway activated by the BMP-9 signaling cascade. It has also been reported that in the absence of Hey1, the cell differentiation regime of the pluripotent MSCs take a chondrogenic route, whereas, the presence of Hey1 enhances the bone matrix mineralization during BMP-9 induced cell differentiation and bone development. Also, there exists a synergy between RUNX2 and Hey1 during BMP-9 induced osteogenic differentiation, wherein the absence of Hey 1 resulted in a significant reduction of RUNX2 expression. This suggests that RUNX2 may be a downstream element of the signaling cascade followed by Hey1, and both play a key role in osteogenic differentiation of MSCs [57].

Connective tissue growth factor (CTGF), is a member of the cysteine-rich multi-modular protein family known as CCN; CCN acronym has been derived from its first three discovered members of the protein family comprising of cysteine-rich angiogenic protein 61 (CYR61), connective tissue growth factor (CTGF), and nephroblastoma overexpressed (NOV). CTGF also plays a key role in the BMP-9 induced signaling pathway along with the development of bone, scar formation or fibrosis, tumorigenesis, embryogenesis, and chondrocyte maturation [103, 108-114]. It is known that skeletal dysmorphism is evident during the absence of CGTF with site-specific aberrations in the formation of bone [112, 115, 116]. The literature states that osteoblast formation from stem cells is regulated jointly by the BMPs and the Wnt signaling pathway [56]. At the onset of BMP-9 induction, the upregulation of CTGF was reported through microarray data. However, the upregulation was diminished to the basal level around day 7. Through gene knockdown studies, the crucial role of CTGF in BMP-9 induced osteogenic differentiation; although the Wnt3A induced differentiation was unhindered. Constitutive expression of CTGF reported inhibition of both BMP-9 as well as Wnt3A osteogenic differentiation. Moreover, the recruitment of MSCs

and cell migration were enhanced with the exogenous expression of CTGF. The upregulation of CTGF by BMP-9 and Wnt3A at the early cell differentiation stages is balanced with its downregulation when adequate preosteoblasts differentiation potential is achieved. The findings signify the presence of tight regulation in the expression of CTGF during osteogenic differentiation from MSCs [56].

3. Role of BMP-9 in Bone Tissue Regeneration

3.1. Non-viral Vector Delivery

Non-viral vectors for the delivery of BMPs have been used considerably over the past twenty years or so. Polymeric materials, mostly cationic, peptides, calcium phosphate, lipids, several inorganic biocompatible nanomaterials have been reported as some of the common types of biomaterial for the delivery of genetic information into the target cell [117]. The positive charge on cationic polymers facilitate the formation of polyplexes with the negatively charged DNA molecules; polyplexes are transferred to the target cells to activate specific signaling pathways required for differentiation [118]. Although, the non-viral vector delivery method poses a disadvantage in the form of low gene transfer efficiency to target cells, the non-viral delivery of BMP-9 stands as a safer alternative to its viral counterpart for orthopaedic applications [119]. Non-viral delivery methods prevent inflammation of surrounding host tissue and/or site morbidity, as compared to the viral delivery techniques [120]. The inclusion of viral vectors into the genome poses risks related to mutagenesis and oncogenesis [121].

Several non-viral delivery methods have been utilized in recent literature, as summarized in Table 2. The peptides derived from BMPs have been used as a low-cost alternative that mimics recombinant BMPs (rhBMPs) in the past [122, 123]. A unique non-viral BMP-9 delivery method was construed using peptide derived from recombinant BMP-9 (pBMP-9) to induce osteogenic differentiation in murine preosteoblasts *in vitro* [124]. Further studies were conducted using a scaffold-based delivery method using chitosan and collagen separately. During *in vitro* BMP-9 release, high performance liquid chromatography (HPLC) revealed that after 10 days of incubation around 45% of the pBMP-9 was released from the chitosan delivery system compared to 75% release of the pBMP-9 from its collagen counterpart; however, both the delivery methods released around 15% each pBMP-9 after 6 h of incubation. This observation may be attributed to the electrostatic attraction between the pBMP-9 and the chitosan/collagen polymer system. Moreover, the possible degradation of the collagen scaffold with time due to attack by metalloproteinases may account for the faster release of pBMP-9 from collagen over the chitosan delivery model. Thus, it should be noted that the transport mechanism or release profile of the pBMP-9 from the polymeric carrier may be dependent on the choice of polymer with regards to its pH, physical structure that also includes the crosslinking strength and isoelectric point. Also, further insight on the scaffold morphology, such as surface roughness or hydrophilicity, or zeta potential, maybe studied for more robust tuning of the release kinetics of the pBMP-9 from natural polymeric constructs. *In vivo* studies on mouse quadricep muscle displayed that only the chitosan delivery system with rhBMP-9 as well as pBMP-9 managed to induce ectopic bone formation within day 24; the calcification/muscle ratio of the BMP-9/chitosan delivery

system was 2.1 to 11.4 times that of the chitosan only control. The ectopic bone formation may have been aided by the inflammatory response triggered by chitosan over collagen; as inflammatory cell actions facilitate bone regeneration [125, 126]. However, a wide mouse-to-mouse variation was reported for the ectopic bone calcification volume. The muscle samples treated with BMP-9 and the chitosan delivery system were analyzed with H&E staining or von Kossa or toluidine blue. It revealed mineralization of both the control rhBMP-9 as well as pBMP-9 samples; concentric circular structures with mineral deposition was reported for the pBMP-9 samples. Immunolabeling studies conducted with antibodies directed against Desmin confirmed that the delivery system with BMP-9 and chitosan invoked disruption of the muscle tissue for the formation of cartilaginous tissue. The pBMP-9/chitosan delivery system treated samples revealed a lamellar bone structure which was surrounded by muscle cells that have been degenerated [126]. However, the optimal dosage of pBMP-9 for bone defect healing is yet to be studied; it may be taken into consideration that the lamellar structure of the ectopic bone formation hints at a newly formed bone that conforms closely with the natural bone. Also, it may be hypothesized that with the existence of a host bone, in the case of a bone defect, the cellular actions leading to new bone formation may be more robust for the pBMP-9 in comparison to the ectopic bone formation in muscles. Another novel study incorporating lipid nanoparticles (LNPs) using histidine modified octadecylamine and pBMP-9 revealed enhanced osteogenic differentiation *in vitro* as well as *in vivo* bone growth in osteoporosis induced ovariectomized (OVX) rat model [127]. The LNPs were characterized and reported to have an approximate size of 100 nm, and they also exhibited stability in a 2% sodium chloride solution. The LNPs also displayed stability in DNase I as well as serum. PEGlylation of the LNPs may be attributed to the stability of the nanoparticles in serum as well as electrolytes; this improves the residence time of the LNPs in blood; also, the possible hydrogen bonding occurring between the ionizable lipid and the pBMP carrier may induce increased LNP stability too. This facilitates the intravenous administration of pBMP-9 via the LNPs, as the bone marrow MSCs are otherwise hard to reach and transfect [127, 128]. Moreover, the LNPs also showed negligible cytotoxicity *in vitro*, using C2C12 cells. The transfection studies carried out with pBMP-9 using von Kossa staining for calcium deposition indicated the osteogenic differentiation potential of the BMP-9 on C2C12 cells, as compared to the naked pDNA transfected cells that showed negative staining. The LNP transfected C2C12 cells were reported to have shown osteoblastic morphology when they reached confluence, as compared to naked pBMP-9 transfected cells. This also displays the influence of the delivery system, LNPs in this case for the transfection potential. Moreover, the transfection efficiency of the LNPs may be attributed to the enhanced endosomal escape that might facilitate improved cellular signaling. In this regard, it may be noted that the amount of PEGlylation plays a crucial role in the endosomal acidification as well as significantly reduce the pBMP-9 uptake by the liver at PEG concentrations less than 2.5 mol%. As shown in Figure 4, high-resolution X-ray radiograph results revealed that in an *in vivo* environment the radiopacity of the femoral and lumbar vertebral bones increased with the LNPs as compared to the control group. Moreover, the hip bone region, especially in the epiphysis and metaphysis regions, displayed trabecular bone growth, as evident from enhanced radiopacity in those regions in the OVX rats. The cortical bone thickness was also reported

to have been increased with a reduction in endosteal diameter for the LNPs, as shown in Figure 4 [127].

Collagen, which is a widely used biomaterial for bone tissue regeneration, has also been reported as an excellent non-viral carrier for BMP-9. A study using a nanohydroxyapatite (nHA)/collagen I (Col1)/multi-walled carbon nanotube (MWCNT) 3D scaffold system loaded with rhBMP-9 has reported very promising results both *in vitro* and *in vivo* with BMMSCs; the scaffold system has been denoted as nHACM, where nHA – nanohydroxyapatite, C – collagen I, and M - multi-walled carbon nanotube [129]. The incorporation of nanofillers, such as nHA and MWCNT, may be noted as enhancers of physical as well as biological properties of scaffolds. Nanofillers induce enhanced mechanical properties such as compressive strength and stiffness to the scaffolds; moreover, these nanofillers are often present in the native bone extracellular matrix (ECM) and they sometimes act as seed crystals for biomineralization, as in the case of nHA. The 3D scaffolds were prepared using lyophilization technique, with 1% wt. MWCNT, 2% (w/v) Col1 that was added with nHA in the ratio of 3:7 (w/w). Cells were observed to have a random attachment profile across the scaffold, as shown in Figure 5 (I). The adequate 3D structure of the composite scaffold with the interconnected porous network may be attributed to the optimal cellular attachment. Moreover, the porous structure of the scaffold also facilitates adequate nutrient transport that enhances the cellular proliferation and growth of filopodia or cytoskeletal extensions. However, it should also be kept in mind that the release of the loaded rhBMP-9 needs to be tuned with the scaffold structure by manipulating its physical and chemical attributes of the chosen biomaterial, crosslinking, pH, etc. The *in vitro* evaluation of the BMP-9 loaded 3D scaffolds using BMMSCs reported significantly higher ALP activity for the sample groups treated with nHACM and nHACM + rhBMP-9, as compared to the control groups. Moreover, Quantitative polymerase chain reaction (qPCR) results displayed OCN, OPN, AND Col1α1 gene expression enhancement with the nHACM + BMP-9 sample group, as compared to the nHACM only group, as shown in Figure 5 (II); thus, highlighting the efficacy of BMP-9 in the late osteogenic marker expression and a viable advantage in osteogenic differentiation *in vitro*. However, it may be highlighted that the utilization of a composite 3D scaffold with Col1 and MWCNT may be attributed more towards the enhanced osteogenic marker expression than just the mere presence of BMP-9 in the osteogenic environment. Thus, the choice of composite scaffold fabrication material is quintessential in obtaining adequate bone regeneration. *In vivo* studies, using Sprague-Dawley rats, on 8 mm critical-sized cranial defects exhibited the intricate advantage of using BMP-9 with the 3D scaffold system. The Hounsfield Unit (HU) data revealed the highest number for the nHACM + BMP-9 group with BMMSCs. Micro Computed Tomography (Micro-CT) data also highlighted the advantage of the BMP-9 loaded scaffold group over the other sample groups in terms of a larger area of new bone formation, as shown in Figure 5 (III). Further, the histology data, as shown in Figure 5 (IV) confirmed these findings on the efficacy of the BMP-9 loaded scaffold system in terms of new bone development as compared to the other sample groups. The presence of BMMSCs along with the BMP-9 loaded composite scaffold may be attributed to the complete closure of the *in vivo* bone defects; the cellular traffic in the vicinity of the bone defect may be the driving potential in this case. Thus, it can be inferred that the optimal bone defect implant may be designed with

stem cell incorporation with the BMP-9 loaded scaffold [129]. Another collagen-based 3D scaffold, nHA/Col-BMP-9/gelatin microsphere (GM), was prepared through a combined fabrication method of mixing, crosslinking, and freeze-drying [130]. GMs were prepared by crosslinking process using glutaraldehyde and Type A gelatin; BMP-9 was encapsulated into the GMs using an emulsion-solvent diffusion technique [130, 131]. These BMP-9 loaded GMs were gently added to the nHA/Col polymer blend, followed by freeze-drying. The use of collagen and nHA may be attributed to their excellent biocompatibility and facilitation in mimicking native bone (ECM). nHA particles also may be a suitable target for borne forming cells during mineralization. *In vitro* release study of the BMP-9 loaded GMs, using ELISA, reported an initial burst release for day 1, followed by a more sustained release profile up to day 13 when it flattened out; the plateau suggested the constant release of BMP-9 from the GMs up to day 21 with a total release amount reaching 95.59 ± 2.82% cumulatively. Cell attachment, using rat BMMSCs, after 6 h of incubation has been reported to be significantly higher for the BMP-9 loaded scaffolds, as compared to its counterparts without BMP-9; however, it has been noted that the scaffolds with BMP-9 went through more freeze drying cycles than the BMP-9 controls thereby providing more opportunity for enhanced porous structure. Also, the overall increase in cell attachment with the scaffold containing groups, compared to the control, suggests that the surface roughness due to the presence of nHA on the scaffold surface is a core scaffold design aspect. Moreover, ALP activity on day 7 and 10 have been reported to be significantly higher for the BMP-9 loaded scaffolds. These findings confirm the efficacy of the BMP-9 loaded scaffold in terms of cell attachment as well as osteogenic differentiation. *In vivo* biocompatibility studies verified the safety and nontoxicity of the scaffolds, as listed in Table 2. The degradation products of the scaffold did not cause any observable tissue irritation, which further infers biocompatibility of the scaffold biomaterial [130]. A guided bone regeneration (GBR) study using rhBMP-9 with deproteinized bovine bone mineral (BO) and collagen barrier membrane (BG) separately in a rabbit GBR model reported increased bone growth in the defects [132]. The new bone formation in rabbit calvarial defects induced by rhBMP-9 using both the delivery systems (BO and BG) were assessed to be comparable and significantly enhanced in comparison to the control groups without rhBMP-9, as inferred from the Micro-CT data. Histological evaluation of the tissue samples confirmed these findings, however, it also revealed that a higher new bone formation was observed around the BO group surrounding the center of the defect area including the BO group that did not have rhBMP-9; angiogenesis was observed only around the BG sites that contained rhBMP-9 along. Histomorphometry evaluation of the tissue samples confirmed the new bone formation potential of both rhBMP-9 containing sample groups. It also revealed the importance of collagen in the rhBMP-9 induced bone formation as more horizontal bone defect closure, higher levels of bone marrow region, and smaller regions of soft/connective tissue were observed for the BG groups containing rhBMP-9. This observation may be explained as the superior adsorption potential of collagen membrane, as compared to BO which is crafted from bioceramic material, that also accounts for a more sustained release of the BMP-9; thus, adequate quantity of BMP-9 was exposed to the incoming bone forming cells over a considerable longer period of time with the application of collagen based scaffold [132]. Similar results have been reported in several studies with the use of rhBMP-9 and collagen that highlight the enhanced BMP-9 adsorption potential of collagen and subsequent

advantage of rhBMP-9 in osteogenesis. Overall, it should be noted that the presence of collagen serves to facilitate an adequate uptake of the BMP-9 along with a sustained release profile; this is an major added advantage of using collagen based scaffolds along with the biomimicry of collagen rich native bone ECM [133-138].

In a study focused on an injectable gel scaffold-based delivery system for rhBMP-9, a thermoresponsive polymer blended gel system with embedded chitosan microparticles was used to study the bone regeneration effect [139]. The study incorporated a blend of methylcellulose and alginate polymers to fabricate the thermosensitive gel system and then loaded with chitosan microparticles that have been coated with rhBMP-9. The incorporation of chitosan microparticles may be inferred as a carrier for the rhBMP-9 along with a possible inflammatory response in the bone defect site that aids in bone defect healing by increasing cellular traffic. The polymeric gel system of methylcellulose and alginate creates a hydrogel-based network for housing the BMP-9 coated chitosan microparticles; the thermosensitive property of methylcellulose being harnessed at physiological temperatures along with crosslinked alginate for initiation of partial gelling during scaffold delivery. The burst release mechanism of the coated rhBMP-9 on the microparticles was regulated by the gel system which was deemed to act as a reservoir for the BMP-9. The release study data, using enzyme-linked immunosorbent assay (ELISA), reported that only 20% of the coated rhBMP-9 was released from the gel scaffold within 24 h, thus, exhibiting a sustained release profile, as shown in Figure 6 (I – A and B). *In vitro* studies on 2D culture using human MSCs (hMSCs) exhibited an increased ALP activity in the presence of rhBMP-9, as compared to the control group without BMP-9, Figure 6 (I C). The expression of ALP, Col1, and OCN has also been reported, by using RT-PCR, to have been upregulated at day 7 with the addition of BMP9, Figure 6 (I – D, E, and F). Thus, osteogenic differentiation of the hMSCs was evident from the ALP activity, as well as the other gene expression upregulation, with the BMP-9 mediation. The mineralization induced by the osteogenic differentiation of the hMSCs were evaluated using Alizarin Red staining on day 14 revealed a more uniform and denser mineral deposition on the sample group with rhBMP-9, as compared to the control group without BMP-9. This observation may be attributed solely to the presence of BMP-9 in combination with the biocompatible hydrogel scaffold. Moreover, the presence of chitosan may be deemed to have played a crucial part in this osteogenic differentiation and biomineralization phase along with BMP-9, however, the microparticles alone with the gel scaffold provided no intrinsic benefit towards mineralization. Bioactivity analysis of the BMP-9 on the coated microparticles reported that the hMSCs attached and proliferated more with the microparticles coated with rhBMP-9, as compared to the control group without BMP-9 at day 3 and 7, thus, highlighting the role of BMP-9 as a cellular cue for attachment and proliferation. Ectopic bone formation at the subcutaneous site was reported to be significantly higher at 4 weeks for the sample groups containing rhBMP-9 with a woven bone-like structure, as compared to the control group without rhBMP-9; the mineral content of the ectopically formed bone was significantly higher for the sample group with rhBMP-9 loaded, as evident from DEXA analysis. Moreover, the presence of rat MSCs along with the BMP-9 loaded gel scaffold did not infer any significant difference to the bone formation profile without cells, but a rigorous bone structure was observed with MSCs present along with the scaffold. Thus, it may be noted that in an ectopic bone formation

model, the presence of stem cells along with the BMP-9 loaded scaffold may cause to accelerate the disruption of muscle tissue and enhance subsequent ossification; however, in the case of bone defects, the presence of cells along with the scaffold may not be very significant. *In vivo* studies on critical-sized rat cranial defects confirmed the efficacy of the rhBMP-9 loaded scaffold system, as compared to the control group. Micro-CT data revealed that at 12 weeks post-surgery, the cranial defects were filled up completely for the rhBMP-9 loaded sample group, as shown in Figure 6 (II – A). The bone volume study results also reported a higher outcome with the rhBMP-9 loaded sample groups, Figure 6 (II – B). Further histology analysis confirmed that the sample group with rhBMP-9 completely closed the cranial defect at 12 weeks, as compared to fibrous connective tissue formation exhibited by the gel only sample group without rhBMP-9 and VEGF. Furthermore, the presence of osteoblasts, osteocytes, and osteoid in the vicinity of the healing bone defect infers the significance of BMP-9 in attracting bone cells along with new bone formation [139].

In vitro studies on bone grafts with rhBMP-9 loading exhibits its potential efficacy in bone grafting techniques using demineralized freeze-dried bone allografts (DFDBAs) and biphasic calcium phosphate (BCP) [140]. The adsorption and release profile of rhBMP-9 is more efficient in BCP than DFDBA. As listed in Table 2, the surface roughness and presence of nano topographies on the BCP particles may be attributed for the enhanced adsorption of rhBMP-9. Moreover, the rough surface of the BCP particles, as compared to the smooth DFDBA surface, may also enhance the cell attachment and subsequent proliferation. The ALP staining assay data highlighted the 7 fold increase in ALP activity with the rhBMP-9 loaded DFDBAs; however, real time-PCR data showed that all DFDBA samples were reported to have shown a downregulation of RUNX2 at day 3 post-seeding. Interestingly, the BCP samples loaded with rhBMP-9 showed a 50 fold increase in ALP activity at day 7 post-seeding, as compared to the control samples. Alizarin red staining results confirmed the osteogenic advantage of rhBMP-9 on both the graft material (DFDBA and BCP) as compared to their control counterparts. The enhancement in osteogenic differentiation with the presence of BCP and rhBMP-9 may be inferred as a result of the superior adsorption of the BMP-9 onto BCP. Since, the conformation of the adsorbed protein also plays a significant role in its release profile, hence comparison of the BCP over DFDBA in terms of protein adsorption may be noted [140]. Another similar study with rhBMP loaded onto porcine collagen membranes have also been reported to have an advantage in terms of osteo-promotive function [141]. The three dimensional structure of the collagen membrane facilitates cell attachment and subsequent proliferation. Furthermore, the additional benefit of coupling BMP-9 with the membrane was revealed through real time-PCR studies as RUNX2 was not influenced by rhBMP-9 loaded collagen membranes, however, ALP and BSP expressions were reported to have been upregulated at day 3 and day 14 respectively. Alizarin red staining again confirmed the increased staining with rhBMP-9 samples as compared to the counterparts in comparison [141].

Fibrin sealants are also known for their use as adhesive tools for bone grafts and coagulants. In an *in vitro* study involving fibrin sealant and rhBMP-9 reported a sustained release of the BMP over 10 days, with around 40% of the original amount of rhBMP-9 remaining after that in the scaffold [142]. The BMP adsorption potential of fibrin sealant may be highlighted through this result that indicates the localized release of BMP-9 over a sustained period;

both maximum adsorption of the BMP, as well as its slow release locally at the defect site, are quintessential factors for regulating osteogenesis. Hence, while using bone marrow derived stromal cell line (ST2) cells, the osteogenic differentiation potential was reported to have been enhanced with the use of rhBMP-9 loaded fibrin sealant scaffold. Moreover, the ALP activity results displayed a 3 fold increase with the incorporation of rhBMP-9 with the fibrin sealant. Also, from RT-PCR results the ALP mRNA and OCN expressions at day 3 post-seeding have been reported to have displayed a 2 and 6 fold increase respectively for the scaffolds containing rhBMP-9; on day 14 post-seeding, BSP and OCN expressions were upregulated by 8 and 5 folds respectively. These results, including the Alizarin red staining enhancement with rhBMP-9 containing scaffolds, confirmed the efficacy of the rhBMP-9 in conjunction with fibrin sealant which may be used more extensively in bone tissue regeneration studies equally [142].

Hyaluronic acid (HA) in conjunction with rhBMP-9 has also been studied *in vitro* with an aim directed towards potential bone defect healing [143]. The hyaluronic acid, crosslinked with butanediol diglycidyl ether, was incorporated with rhBMP-9 and the release kinetics showed a burst release of around 30% in 24 h, followed by a sustained release for the next 10 days. At the end of the release period, around 35% of the original amount of rhBMP-9 added to the scaffold was reported to have been left unreleased from the scaffold. Hence, it may be noted that crosslinked HA scaffolds were adequate in providing a suitable matrix for holding the growth factor. Moreover, the sustained release profile of the BMP may be inferred as the reason for the superior osteogenic differentiation potential of the BMP loaded HA scaffold. Seven days post-seeding, the HA scaffolds containing rhBMP-9 showed increased ALP staining and enhanced expressions of Col1 and ALP using RT-PCR. The late osteogenic marker OCN was reported with enhanced expression at day 14 for the rhBMP-9 containing HA scaffolds, as compared to the control group; 4 fold increase for rhBMP-9 + HA as compared to a 2 fold increase for HA only. Alizarin red staining also reported a 4 fold increase in staining with the addition of rhBMP-9 to the HA scaffolds. These results are evidence of the superior osteogenic potential induced by rhBMP-9 on the HA scaffolds. Moreover, HA alone has also been reported to facilitate adequate osteogenic differentiation as listed in Table 2 [143].

In addition to the regular non-viral methods of introducing BMP-9 to the target site, such as adsorption and encapsulation in bulk polymer matrix or microsphere, other novel techniques have also been formulated for BMP-9 delivery. Such a procedure involves using a sonoporation technique involving naked DNA encoding *in vivo* of rhBMP9 [144]. The *in vivo* study was designed to analyze the ectopic bone formation through direct injection of rhBMP-9 encapsulated inside a perfluoro propane-filled albumin microbubble/microsphere. The microbubble method incorporates the collapse of the bubble with the application of ultrasound, and subsequent release of its contents in microjets that are more effective in cell permeability [144, 145]. The study also used electroporation as a comparison to the hypothesized sonoporation technique. The ectopic bone volume data revealed that the electroporation and sonoporation techniques achieved 3.12 ± 0.8 mm^3 and 0.9 ± 0.17 mm^3 respectively for the rhBMP-9 induced samples. Moreover, the bone volume density of sonoporation and electroporation were reported as 0.7 ± 0.09 and 0.27 ± 0.02 respectively; bone mineral density with respect to hydroxyapatite was found to be 793.51 ± 68.44 mg HA

per cm^3 and 604.47±14.28 mg HA per cm^3 for sonoporation and electroporation respectively. Micro-CT-and histology studies displayed that only rhBMP-9 delivered sample groups exhibited formation of the ectopic bone in the muscle tissue during both sonoporation as well as electroporation methods. Representative images are shown in Figure 7 [144]. Another study incorporated with human BMP-9 (hBMP9) transfected human MSCs (hMSCs) using nucleofection through a novel electro-permeabilization technique [146]. This technique reported cell viability of 53.6±2.5% with 68.2±4.1% average efficiency in gene delivery for the enhanced green fluorescent protein (EGFP) nucleofected hMSCs. A significant enhancement in calcium deposition was observed from the hBMP-9 nucleofected hMSCs, as compared to the control EGFP nucleofected ones. The transgene expressions also have been reported to have lasted longer than 14 days, and it diminished to a very low amount at around day 21 post-nucleofection; however, it was studied only with hBMP-2 nucleofected samples. *In vivo* studies with hBMP-9 nucleofected hMSCs revealed ectopic bone formation at 4 weeks in the distal part of the thigh muscle in a nonobese diabetic/severe combined immunodeficiency (NOD/SCID) mouse model. The ectopic boney mass revealed mature bone tissue comprising of trabecular bone and bone marrow [146].

3.2. Viral Vector Delivery

Growth factors, such as BMPs, are delivered to the stem cells by transfecting with viruses. Some of the commonly used viruses for viral delivery systems include adenoviruses, adeno-associated viruses, retroviruses, and lentiviruses. Adenovirus vectors are more commonly reported as have been used to carry plasmids that facilitate the encoding of BMPs [148] [149]. A combination of the viral vector and biomaterial, known as gene activated matrix (GAM), has also been reported for bone tissue regeneration studies. The BMP-plasmid viral vectors are loaded into the biomaterial, such as chitosan, calcium phosphate, collagen, etc., which may be implanted into the bone defect site [150]. The advantages of viral vector delivery of growth factors, such as BMPs, include local expression of the BMP at the defect site. Also, the viral vector delivery method opens up the chances for the synthesis of the BMP intra-cellularly, thereby leading to the activation of therapeutic signaling cascades in cell signaling. The viral vector delivery method for BMPs also transfers a nascent form of the protein that is free of contamination from antigenic molecules. Moreover, regulation of transgene expression may be controlled with the viral vector delivery technique along with an extended length of time for expression of BMPs [151].

A biodegradable scaffold-based delivery route was inducted using poly(polyethyleneglycol citrate-co-N-isopropylacrlamide) (PPCN), synthesized by sequential polycondensation and radical polymerization, and blended with gelatin (PPCNG). PPCN shows a lower critical solution temperature of 26 °C, and it forms a gel at 30 °C. Thus, the thermosensitivity of gelling for the scaffold system is adequate at physiological temperature. Moreover, the addition of gelatin to PPCN adds several benefits, such as neovascularization, uniform cell distribution, etc., to the bone regeneration process, as listed in Table 3. BMP-9 stimulated MSCs using adenoviral vector gene therapy were applied for the repair of the bone defect [152]. The study reported that the incorporation of gelatin resulted in increased adhesion and survival of cells within the gel scaffold. BMP-9 was used to induce differentiation of immortalized mouse embryonic fibroblasts (iMEFs). *In vitro* study results highlighted the

significant advantage in terms of cell adhesion, proliferation, survival as well as increased transgene expression in the 3D culture. Also, *in vivo* study using PPCNG results showed that BMP-9 stimulated iMEFs underwent osteogenic differentiation. Ectopic bone formation in an *in vivo* mouse model in the form of trabecular bone-like structures with vascularization has been reported. Histological results revealed that the PPCNG scaffold with iMEFs exhibited enhanced vascularization among the formed bone-like structures, as compared to the control group; the VEGF staining for PPCNG group was higher than the control group. The neovascularization potential of the PPCNG scaffold may be attributed to the gelatin component. Moreover, the degradation of the PPCN thermoresponsive polymer becomes significant at 3 weeks with complete resorption at around 4 – 5 weeks [152]. Another similar study using thermoresponsive PPCNG and murine-derived calvarial mesenchymal progenitor cells (iCALs), that was transduced by Adenoviral BMP-9 (Ad-BMP-9), reported adequate osseointegration and mature bone formation [153]. Using Micro-CT, *in vivo* calvarial critical-size defects treated with PPCNG scaffold seeded with iCALs and infected with Ad-BMP-9 displayed a significantly higher defect gap closure, as compared to the control group in the absence of Ad-BMP-9. Histology data of the calvarial defects confirmed the same scenario in BMP-9 mediated new bone formation [153]. Also, studies using iMADs infected with Ad-BMP-9 and PPCNG have reported adequate healing of critical-sized calvarial bone defects [154]. The PPCNG scaffolds mixed with Ad-BMP-9 infected iMADs were injected into the bone defects. At 12 weeks, Micro-CT and histological analysis revealed that BMP-9 mediated defect healing was significantly higher than the control groups; approximately 27% of the bone defect was healed by the scaffold group containing BMP-9, as compared to approximately 10% for the control group without BMP-9. Thus, the osteogenesis potential of the PPCNG scaffold is enhanced by the incorporation of Ad-BMP-9 infected iMADs [154]. These studies highlighted the benefit of using PPCN as an injectable thermoresponsive polymer. Moreover, the addition of gelatin in varying quantities can be noted as a beneficial modification to the PPCN polymer network which further aids in the bone regeneration process, especially in the promotion of angiogenesis during bone defect healing.

Another study using the adenoviral route for delivery of BMP-9 incorporated seeding with gelatin-derived graphene and silicate nanosheets Laponite (GL) porous scaffolds and powder separately [155]. As listed in Table 3, there is an enhancement of the thermal stability of gelatin with complexation with Laponite nanosheets. Moreover, the addition of graphene sheets may be attributed as a step to promote osteogenic differentiation. Further, it may be discussed that the presence of graphene sheets also provides a rough and adequately stiff structure with nano topographies, which are essential for cell attachment as well as proliferation. This was evident from representative images that showed elongated morphology on the attached iMEF and iMAD cells. Also, the ALP activity was found to be enhanced with the iMEFs infected with Ad-BMP-9, whereas lower ALP activity was observed while using immortalized mouse adipose-derived cells (iMADs). This finding may be attributed to the fact that iMADs are already differentiated more than iMEFs, thus, BMP-9 induce osteogenic differentiation reduces ALP activity which is an early osteogenic marker; negative ALP activity was seen in the case of GL powder without Ad-BMP-9. Alizarin red staining also displayed an enhancement of mineralization with both cell lines,

iMEFs and iMADs, that have been infected with Ad-BMP-9; no such staining was observed in the absence of Ad-BMP-9. *In vivo* studies revealed ectopic bone formation in the form of a trabecular bone structure for the BMP-9 transduced iMEFs with GL powder, as shown in Figure 8 (I – A(a), B(a, b, and c)); although other BMP-9 induced sample groups without GL powder also resulted in a robust bone formation, Figure 8 (I – A(b)) [155].

Coralline hydroxyapatite (CHA) is a material which is usually synthesized by the technique of hydrothermic conversion of sea coral hydroxyapatite to calcium carbonate exoskeletons. CHA scaffolds seeded with rat dental follicle stem cells (rDFCs) and transfected with Ad-BMP-9 has exhibited increased ALP staining, as compared to the control group with no BMP-9 transfection [156]. The highly porous structure of CHA scaffolds, as listed in Table 3, may be noted as a huge benefit in cell attachment, proliferation, and subsequent osteogenic differentiation. RT-PCR data revealed that the ALP mRNA was upregulated on days 5 and 7; Osx expression was also enhanced on day 5, 7, and 9. The late osteogenic marker OPN showed on day 7 and day 9. Alizarin red staining at day 14 also confirmed the efficacy of the BMP-9 transfected rDFCs seeded scaffold. *In vivo* studies, as shown in Figure 8 (II), with rat alveolar bone defects displayed significantly higher new bone formation with vascularization with the BMP-9 transduced cell-scaffold implant group, as compared to all other groups without BMP-9 mediation, at 6 weeks post-implantation. The presence of rDFCs in the scaffold may be explained as a reason to activate adjacent host osteoblasts around the bone defect. Thus, the synergistic osteogenic activity of rDFCs and CHA was significantly highlighted, in addition to the mediation governed by BMP-9. The bone volume Figure 8 (II - E), area of new bone formation Figure 8 (II – D), and new bone volume over total bone volume ratio Figure 8 (II – F) have been reported as significantly higher for the BMP-9 infected rDFCs containing CHA scaffold group; numerous new bone structure was seen around the CHA scaffolds BMP-9 infected rDFCs Figure 8 (II – B(h)), in comparison to more of fibrous connective tissue formation around the CHA scaffolds Figure 8 (II – B(e, f, and g)). These results proved the significant importance BMP-9 holds in a viral vector mediated 3D scaffold system [156]. Another similar study using rDFCs transfected by Ad-BMP-9 in a Matrigel scaffold promotes osteogenic differentiation as well as ectopic bone formation [157]. Matrigel is derived from basement membrane proteins from Engelbreth-Holm-Swarm tumors. Matrigel provides a 3D structure that provides an adequate extracellular matrix for bone regeneration. Moreover, the presence of angiogenic factors in Matrigel should be noted as an additional cue for promoting adequate vascularization during bone defect healing. The rDFCs that were infected with Ad-BMP-9 showed upregulation of osteogenic markers Dlx5, OPN, Osx, and Runx2 on days 3 and 5. Dlx5, Osx, and Runx2 were reported to have been elevated on day 3 which started decreasing gradually till day 5. OPN expression started increasing from day 3 to day 5 with BMP-9 transfection. Further, the rDFCs in Matrigel exhibited spheroid growth at day 7; spheroids are aggregates formed by progenitor/stem cells which deliver the therapeutic advantage of considerably higher resistance to apoptosis and act as a positive factor in the enhancement of differentiation potential and pluripotency marker gene upregulation. These results showing enhanced cell activity and osteogenic differentiation may be noted as the display of biocompatibility of Matrigel. Also, alizarin red staining analysis revealed the calcium deposition enhancement due to BMP-9 mediation, as compared to the control

groups without BMP-9. *In vivo* studies on ectopic bone formation at 6 weeks with subcutaneous injection in athymic nude mice. Micro-CT analysis of the harvested tissues revealed increased bone volume and surface with the BMP-9 transduced rDFCs with Matrigel scaffold. Immunohistochemical staining experiments exhibited the presence of osteoid matrix in the harvested tissues. These results confirm the enhanced osteogenic differentiation potential of the BMP-9 transduced rDFCs with Matrigel. Histology analysis of the tissues revealed thicker trabecular bone structures that were found uniformly in the bone mass, compared to the peripheral trabecular bone in the BMP-9 transduced sample group without Matrigel. Trichrome staining confirmed the H&E staining results that Ad-BMP-9 transfected rDFCs with Matrigel induced more mature bone formation at 6 weeks compared with the BMP-9 mediated group without Matrigel. These results are sufficient confirmation to endorse Matrigel as a beneficial scaffold material for bone defect healing, preferably with BMP-9 mediated stem cell osteogenic differentiation [157].

4. Conclusion

The regeneration of bone tissue in a defect model is governed by a multitude of factors. The osteogenic differentiation potential of the scaffold environment at the defect site is one of the key parameters governing the bone regeneration process. In this regard, BMP-9 mediated osteogenic differentiation has shown to be beneficial over scenarios without BMP-9 mediation. Also, the inclusion of a 3D scaffold system has shown to be advantageous for bone regeneration, especially in the non-viral delivery of BMP-9. As stated in the literature, the scaffold properties such as porosity, mechanical stiffness, roughness, etc., are also key factors in regulating cell attachment and proliferation. These physical cues offered by 3D constructs along with adequate BMP-9 mediation enhances the bone-forming potential of the scaffold system. Moreover, the thermoresponsive nature of the scaffold system renders the injectability of the scaffold at room temperature with subsequent gelation at physiological temperature. The Smad pathway that regulates the BMP-9 signaling cascade is not affected by Noggin. This holds one of the major advantages over most of the other BMPs known. The Noggin resistance of BMP-9 allows the BMP-9 mediated signaling pathway to intrinsically facilitate the osteogenic differentiation of various stem cells that render the bone formation process. It was also evident from some of the studies that the critical-sized calvarial defects in rats were reported to have been efficiently closed in the presence of rhBMP-9 in a non-viral delivery model. The non-viral delivery system for BMP-9 again is a breakthrough that has reported BMP-9 mediated adequate new bone formation at a low dosage in several recent studies. Efficacy of application of low dosage of BMP-9 hints that the optimization of the release kinetics of the BMP over a localized defect area is one of the key parameters for governing BMP-9 mediated bone regeneration; often higher dosage of BMP incorporation may be required when there is a potential for loss in BMP mediated osteogenic differentiation efficiency due to lower BMP uptake and/or a faster release of the BMP from the carrier. Future studies may venture into various biopolymer composites, along with nanofiller incorporation, that provides adequate physical cues as well as extensive BMP-9 adsorption and sustained release over time. Injectable porous scaffold systems with sustained release design for rhBMP-9 show potential for adequate new bone formation in both *in vitro* and *in vivo* conditions.

Acknowledgments

The authors would like to acknowledge funding support from the National Institutes of Health (R01DE023356).

References

[1]. Downey PA, Siegel MI, Bone biology and the clinical implications for osteoporosis, Physical therapy 86(1) (2006) 77–91. [PubMed: 16386064]

[2]. Buckwalter J, Glimcher M, Cooper R, Recker R, Bone biology, J Bone Joint Surg Am 77(8) (1995) 1256–1275.

[3]. Florencio-Silva R, Sasso G.R.d.S., Sasso-Cerri E, Simões MJ, Cerri PS, Biology of bone tissue: structure, function, and factors that influence bone cells, BioMed research international 2015 (2015).

[4]. Robling AG, Castillo AB, Turner CH, Biomechanical and molecular regulation of bone remodeling, Annu. Rev. Biomed. Eng 8 (2006) 455–498. [PubMed: 16834564]

[5]. Datta H, Ng W, Walker J, Tuck S, Varanasi S, The cell biology of bone metabolism, Journal of clinical pathology 61(5) (2008) 577–587. [PubMed: 18441154]

[6]. Miller SC, de Saint-Georges L, Bowman B, Jee W, Bone lining cells: structure and function, Scanning microscopy 3(3) (1989) 953. [PubMed: 2694361]

[7]. Clarke B, Normal bone anatomy and physiology, Clinical journal of the American Society of Nephrology 3(Supplement 3) (2008) S131–S139. [PubMed: 18988698]

[8]. Karsenty G, Kronenberg HM, Settembre C, Genetic control of bone formation, Annual Review of Cell and Developmental 25 (2009) 629–648.

[9]. Teitelbaum SL, Osteoclasts: what do they do and how do they do it?, The American journal of pathology 170(2) (2007) 427–435. [PubMed: 17255310]

[10]. Bonewald LF, The amazing osteocyte, Journal of bone and mineral research 26(2) (2011) 229–238. [PubMed: 21254230]

[11]. Sims NA, Gooi JH, Bone remodeling: Multiple cellular interactions required for coupling of bone formation and resorption, Seminars in cell & developmental biology, Elsevier, 2008, pp. 444–451.

[12]. Matsuo K, Irie N, Osteoclast–osteoblast communication, Archives of biochemistry and biophysics 473(2) (2008) 201–209. [PubMed: 18406338]

[13]. Amini AR, Laurencin CT, Nukavarapu SP, Bone tissue engineering: recent advances and challenges, Critical Reviews™ in Biomedical Engineering 40(5) (2012).

[14]. O'Keefe RJ, Mao J, Bone tissue engineering and regeneration: from discovery to the clinic—an overview, Tissue engineering part B: reviews 17(6) (2011) 389–392. [PubMed: 21902614]

[15]. Bao CLM, Teo EY, Chong MS, Liu Y, Choolani M, Chan JK, Advances in bone tissue engineering, Regenerative Medicine and Tissue Engineering, IntechOpen 2013.

[16]. Parvizi J, High Yield Orthopaedics E-Book, Elsevier Health Sciences2010.

[17]. Baroli B, From natural bone grafts to tissue engineering therapeutics: brainstorming on pharmaceutical formulative requirements and challenges, Journal of pharmaceutical sciences 98(4) (2009) 1317–1375. [PubMed: 18729202]

[18]. Mishra R, Bishop T, Valerio IL, Fisher JP, Dean D, The potential impact of bone tissue engineering in the clinic, Regenerative medicine 11(6) (2016) 571–587. [PubMed: 27549369]

[19]. Dimitriou R, Jones E, McGonagle D, Giannoudis PV, Bone regeneration: current concepts and future directions, BMC medicine 9(1) (2011) 66. [PubMed: 21627784]

[20]. Yaszemski MJ, Payne RG, Hayes WC, Langer R, Mikos AG, Evolution of bone transplantation: molecular, cellular and tissue strategies to engineer human bone, Biomaterials 17(2) (1996) 175–185. [PubMed: 8624394]

[21]. Finkemeier CG, Bone-grafting and bone-graft substitutes, JBJS 84(3) (2002) 454–464.

[22]. Banwart JC, Asher MA, Hassanein RS, Iliac crest bone graft harvest donor site morbidity. A statistical evaluation, Spine 20(9) (1995) 1055–1060. [PubMed: 7631235]

[23]. Ebraheim NA, Elgafy H, Xu R, Bone-graft harvesting from iliac and fibular donor sites: techniques and complications, JAAOS-Journal of the American Academy of Orthopaedic Surgeons 9(3) (2001) 210–218.

[24]. St TJ, Vaccaro AR, Sah AP, Schaefer M, Berta SC, Albert T, Hilibrand A, Physical and monetary costs associated with autogenous bone graft harvesting, American journal of orthopedics (Belle Mead, NJ) 32(1) (2003) 18–23.

[25]. Gupta A, Main BJ, Taylor BL, Gupta M, Whitworth CA, Cady C, Freeman JW, El-Amin SF III, In vitro evaluation of three-dimensional single-walled carbon nanotube composites for bone tissue engineering, Journal of Biomedical Materials Research Part A 102(11) (2014) 4118–4126. [PubMed: 24443220]

[26]. Holzmann P, Niculescu-Morzsa E, Zwickl H, Halbwirth F, Pichler M, Matzner M, Gottsauner-Wolf F, Nehrer S, Investigation of bone allografts representing different steps of the bone bank procedure via the CAM-model, ALTEX-Alternatives to animal experimentation 27(2) (2010) 97–103.

[27]. Urist MR, Bone: formation by autoinduction, Science 150(3698) (1965) 893–899. [PubMed: 5319761]

[28]. Wagner DO, Sieber C, Bhushan R, Börgermann JH, Graf D, Knaus P, BMPs: from bone to body morphogenetic proteins, American Association for the Advancement of Science, 2010.

[29]. Brand RA, Marshall R. Urist, 1914–2001, Clinical Orthopaedics and Related Research® 467(12) (2009) 3049. [PubMed: 19727990]

[30]. Wang RN, Green J, Wang Z, Deng Y, Qiao M, Peabody M, Zhang Q, Ye J, Yan Z, Denduluri S, Bone Morphogenetic Protein (BMP) signaling in development and human diseases, Genes & diseases 1(1) (2014) 87–105. [PubMed: 25401122]

[31]. Luo J, Sun MH, Kang Q, Peng Y, Jiang W, Luu HH, Luo Q, Park JY, Li Y, Haydon RC, Gene therapy for bone regeneration, Current gene therapy 5(2) (2005) 167–179. [PubMed: 15853725]

[32]. Luther G, R Wagner E, Zhu G, Kang Q, Luo Q, Lamplot J, Bi Y, Luo X, Luo J, Teven C, BMP-9 induced osteogenic differentiation of mesenchymal stem cells: molecular mechanism and therapeutic potential, Current gene therapy 11(3) (2011) 229–240. [PubMed: 21453282]

[33]. Deng Z-L, Sharff KA, Tang N, Song W-X, Luo J, Luo X, Chen J, Bennett E, Reid R, Manning D, Regulation of osteogenic differentiation during skeletal development, Front Biosci 13(1) (2008) 2001–2021. [PubMed: 17981687]

[34]. Kang Q, Song W-X, Luo Q, Tang N, Luo J, Luo X, Chen J, Bi Y, He B-C, Park JK, A comprehensive analysis of the dual roles of BMPs in regulating adipogenic and osteogenic differentiation of mesenchymal progenitor cells, Stem cells and development 18(4) (2009) 545–558. [PubMed: 18616389]

[35]. David L, Mallet C, Keramidas M, Lamandé N, Gasc J-M, Dupuis-Girod S, Plauchu H, Feige J-J, Bailly S, Bone morphogenetic protein-9 is a circulating vascular quiescence factor, Circulation research 102(8) (2008) 914–922. [PubMed: 18309101]

[36]. Song JJ, Celeste AJ, Kong F-M, Jirtle RL, Rosen V, Thies RS, Bone morphogenetic protein-9 binds to liver cells and stimulates proliferation, Endocrinology 136(10) (1995) 4293–4297. [PubMed: 7664647]

[37]. Mostafa S, Pakvasa M, Coalson E, Zhu A, Alverdy A, Castillo H, Fan J, Li A, Feng Y, Wu D, The wonders of BMP9: from mesenchymal stem cell differentiation, angiogenesis, neurogenesis, tumorigenesis, and metabolism to regenerative medicine, Genes & Diseases 6(3) (2019) 201–223. [PubMed: 32042861]

[38]. Kowalczewski CJ, Saul J.M.J.F.i.p., Biomaterials for the delivery of growth factors and other therapeutic agents in tissue engineering approaches to bone regeneration, 9 (2018) 513.

[39]. El Bialy I, Jiskoot W, Nejadnik M.R.J.P.r., Formulation, delivery and stability of bone morphogenetic proteins for effective bone regeneration, 34(6) (2017) 1152–1170.

[40]. Blackwood KA, Bock N, Dargaville TR, Ann Woodruff M.J.I.J.o.P.S., Scaffolds for growth factor delivery as applied to bone tissue engineering, 2012 (2012).

[41]. Romagnoli C, D'Asta F, Brandi M.L.J.C.c.i.m., b. metabolism, Drug delivery using composite scaffolds in the context of bone tissue engineering, 10(3) (2013) 155.

[42]. Kargozar S, Mozafari M, Hamzehlou S, Brouki Milan P, Kim H-W, Baino FJAS, Bone tissue engineering using human cells: a comprehensive review on recent trends, current prospects, and recommendations, 9(1) (2019) 174.

[43]. Kargozar S, Hashemian SJ, Soleimani M, Milan PB, Askari M, Khalaj V, Samadikuchaksaraie A, Hamzehlou S, Katebi AR, Latifi NJMS, E. C, Acceleration of bone regeneration in bioactive glass/gelatin composite scaffolds seeded with bone marrow-derived mesenchymal stem cells over-expressing bone morphogenetic protein-7, 75 (2017) 688–698.

[44]. Mantripragada VP, Jayasuriya ACJMS,E. C, Bone regeneration using injectable BMP-7 loaded chitosan microparticles in rat femoral defect, 63 (2016) 596–608.

[45]. Wang Y, Hong S, Li M, Zhang J, Bi Y, He Y, Liu X, Nan G, Su Y, Zhu G, Noggin resistance contributes to the potent osteogenic capability of BMP9 in mesenchymal stem cells, Journal of Orthopaedic Research 31(11) (2013) 1796–1803. [PubMed: 23861103]

[46]. Ghodadra N, Singh K.J.B.t., therapy, Recombinant human bone morphogenetic protein-2 in the treatment of bone fractures, 2(3) (2008) 345.

[47]. Liao J, Wei Q, Zou Y, Fan J, Song D, Cui J, Zhang W, Zhu Y, Ma C, Hu XJCP, Biochemistry, Notch signaling augments BMP9-induced bone formation by promoting the osteogenesis-angiogenesis coupling process in mesenchymal stem cells (MSCs), 41(5) (2017) 1905–1923.

[48]. Faßbender M, Minkwitz S, Strobel C, Schmidmaier G, Wildemann B.J.I.j.o.m.s., Stimulation of bone healing by sustained bone morphogenetic protein 2 (BMP-2) delivery, 15(5) (2014) 8539–8552.

[49]. Cecchi S, Bennet SJ, Arora M.J.J.o.o.t., Bone morphogenetic protein-7: Review of signalling and efficacy in fracture healing, 4 (2016) 28–34.

[50]. Friedlander G, Perry C, Cole JJJBJS, Osteogenic protein-1 in the treatment of tibial nonunions, 83 5151–5158.

[51]. Niu W, Wang Y, Liu Y, Zhang B, Liu M, Luo Y, Zhao P, Zhang Y, Wu H, Ma LJAH, Starch-derived absorbable polysaccharide hemostat enhances bone healing via BMP-2 protein, 119(3) (2017) 257–263.

[52]. Yan S, Zhang R, Wu K, Cui J, Huang S, Ji X, An L, Yuan C, Gong C, Zhang LJG, diseases, Characterization of the essential role of bone morphogenetic protein 9 (BMP9) in osteogenic differentiation of mesenchymal stem cells (MSCs) through RNA interference, 5(2) (2018) 172–184.

[53]. Cheng H, Jiang W, Phillips FM, Haydon RC, Peng Y, Zhou L, Luu HH, An N, Breyer B, Vanichakarn P, Osteogenic activity of the fourteen types of human bone morphogenetic proteins (BMPs), JBJS 85(8) (2003) 1544–1552.

[54]. Kang Q, Sun MH, Cheng H, Peng Y, Montag A, Deyrup A, Jiang W, Luu H, Luo J, Szatkowski J, Characterization of the distinct orthotopic bone-forming activity of 14 BMPs using recombinant adenovirus-mediated gene delivery, Gene therapy 11(17) (2004) 1312–1320. [PubMed: 15269709]

[55]. Peng Y, Kang Q, Luo Q, Jiang W, Si W, Liu BA, Luu HH, Park JK, Li X, Luo J, Inhibitor of DNA binding/differentiation helix-loop-helix proteins mediate bone morphogenetic protein-induced osteoblast differentiation of mesenchymal stem cells, Journal of Biological Chemistry 279(31) (2004) 32941–32949.

[56]. Luo Q, Kang Q, Si W, Jiang W, Park JK, Peng Y, Li X, Luu HH, Luo J, Montag AG, Connective tissue growth factor (CTGF) is regulated by Wnt and bone morphogenetic proteins signaling in osteoblast differentiation of mesenchymal stem cells, Journal of Biological Chemistry 279(53) (2004) 55958–55968.

[57]. Sharff KA, Song W-X, Luo X, Tang N, Luo J, Chen J, Bi Y, He B-C, Huang J, Li X, Hey1 basic helix-loop-helix protein plays an important role in mediating BMP9-induced osteogenic differentiation of mesenchymal progenitor cells, Journal of Biological Chemistry 284(1) (2009) 649–659.

[58]. Zhang J, Weng Y, Liu X, Wang J, Zhang W, Kim SH, Zhang H, Li R, Kong Y, Chen X, Endoplasmic reticulum (ER) stress inducible factor cysteine-rich with EGF-like domains 2 (Creld2) is an important mediator of BMP9-regulated osteogenic differentiation of mesenchymal stem cells, PloS one 8(9) (2013).

[59]. Huang E, Zhu G, Jiang W, Yang K, Gao Y, Luo Q, Gao JL, Kim SH, Liu X, Li M, Growth hormone synergizes with BMP9 in osteogenic differentiation by activating the JAK/STAT/IGF1 pathway in murine multilineage cells, Journal of Bone and Mineral Research 27(7) (2012) 1566–1575. [PubMed: 22467218]

[60]. Tang N, Song WX, Luo J, Luo X, Chen J, Sharff KA, Bi Y, He BC, Huang JY, Zhu GH, BMP-9-induced osteogenic differentiation of mesenchymal progenitors requires functional canonical Wnt/β-catenin signalling, Journal of cellular and molecular medicine 13(8b) (2009) 2448–2464. [PubMed: 19175684]

[61]. Chen L, Jiang W, Huang J, He BC, Zuo GW, Zhang W, Luo Q, Shi Q, Zhang BQ, Wagner ER, Insulin-like growth factor 2 (IGF-2) potentiates BMP-9-induced osteogenic differentiation and bone formation, Journal of Bone and Mineral Research 25(11) (2010) 2447–2459. [PubMed: 20499340]

[62]. Zhang H, Li L, Dong Q, Wang Y, Feng Q, Ou X, Zhou P, He T, Luo J, Activation of PKA/CREB signaling is involved in BMP9-induced osteogenic differentiation of mesenchymal stem cells, Cellular Physiology and Biochemistry 37(2) (2015) 548–562. [PubMed: 26328889]

[63]. Li R, Zhang W, Cui J, Shui W, Yin L, Wang Y, Zhang H, Wang N, Wu N, Nan G, Targeting BMP9-promoted human osteosarcoma growth by inactivation of notch signaling, Current cancer drug targets 14(3) (2014) 274–285. [PubMed: 24605944]

[64]. Wei Z, Salmon RM, Upton PD, Morrell NW, Li W, Regulation of bone morphogenetic protein 9 (BMP9) by redox-dependent proteolysis, Journal of Biological Chemistry 289(45) (2014) 31150–31159.

[65]. Miyazono K, Kamiya Y, Morikawa M, Bone morphogenetic protein receptors and signal transduction, The journal of biochemistry 147(1) (2010) 35–51. [PubMed: 19762341]

[66]. Massagué J, TGF-β signal transduction, Annual Reviews 4139 El Camino Way, PO Box 10139, Palo Alto, CA 94303-0139, USA, 1998.

[67]. Wrana JL, Attisano L, The smad pathway, Cytokine & growth factor reviews 11(1-2) (2000) 5–13. [PubMed: 10708948]

[68]. Luo J, Tang M, Huang J, He B-C, Gao J-L, Chen L, Zuo G-W, Zhang W, Luo Q, Shi Q, TGFβ/BMP type I receptors ALK1 and ALK2 are essential for BMP9-induced osteogenic signaling in mesenchymal stem cells, Journal of Biological Chemistry 285(38) (2010) 29588–29598.

[69]. Wu N, Zhao Y, Yin Y, Zhang Y, Luo J, Identification and analysis of type II TGF-β receptors in BMP-9-induced osteogenic differentiation of C3H10T1/2 mesenchymal stem cells, Acta Biochim Biophys Sin 42(10) (2010) 699–708. [PubMed: 20801928]

[70]. Furukawa F, Matsuzaki K, Mori S, Tahashi Y, Yoshida K, Sugano Y, Yamagata H, Matsushita M, Seki T, Inagaki Y, p38 MAPK mediates fibrogenic signal through Smad3 phosphorylation in rat myofibroblasts, Hepatology 38(4) (2003) 879–889. [PubMed: 14512875]

[71]. Watanabe H, de Caestecker MP, Yamada Y, Transcriptional cross-talk between Smad, ERK1/2, and p38 mitogen-activated protein kinase pathways regulates transforming growth factory-β-induced aggrecan gene expression in chondrogenic ATDC5 cells, Journal of Biological Chemistry 276(17) (2001) 14466–14473.

[72]. Hough C, Radu M, Doré JJ, Tgf-beta induced Erk phosphorylation of smad linker region regulates smad signaling, PloS one 7(8) (2012).

[73]. Xu D.-j., Zhao Y.-z., Wang J, He J.-w., Weng Y.-g., Luo J.-y., Smads, p38 and ERK1/2 are involved in BMP9-induced osteogenic differentiation of C3H10T1/2 mesenchymal stem cells, BMB reports 45(4) (2012) 247–252. [PubMed: 22531136]

[74]. Valenzuela DM, Economides AN, Rojas E, Lamb TM, Nunez L, Jones P, Lp N, Espinosa R, Brannan CI, Gilbert DJ, Identification of mammalian noggin and its expression in the adult nervous system, Journal of Neuroscience 15(9) (1995) 6077–6084. [PubMed: 7666191]

[75]. Zimmerman LB, De Jesús-Escobar JM, Harland RM, The Spemann organizer signal noggin binds and inactivates bone morphogenetic protein 4, Cell 86(4) (1996) 599–606. [PubMed: 8752214]

[76]. Smith WC, Harland RM, Expression cloning of noggin, a new dorsalizing factor localized to the Spemann organizer in Xenopus embryos, Cell 70(5) (1992) 829–840. [PubMed: 1339313]

[77]. Devlin R, Du Z, Pereira R, Kimble R, Economides A, Jorgetti V, Canalis E, Skeletal overexpression of noggin results in osteopenia and reduced bone formation, Endocrinology 144(5) (2003) 1972–1978. [PubMed: 12697704]

[78]. Groppe J, Greenwald J, Wiater E, Rodriguez-Leon J, Economides AN, Kwiatkowski W, Affolter M, Vale WW, Belmonte JCI, Choe S, Structural basis of BMP signalling inhibition by the cystine knot protein Noggin, Nature 420(6916) (2002) 636–642. [PubMed: 12478285]

[79]. Aspenberg P, Jeppsson C, Economides AN, The bone morphogenetic proteins antagonist Noggin inhibits membranous ossification, Journal of Bone and Mineral Research 16(3) (2001) 497–500. [PubMed: 11277267]

[80]. Li J, Li H, Sasaki T, Holman D, Beres B, Dumont R, Pittman D, Hankins G, Helm G, Osteogenic potential of five different recombinant human bone morphogenetic protein adenoviral vectors in the rat, Gene therapy 10(20) (2003) 1735–1743. [PubMed: 12939640]

[81]. Khorsand B, Elangovan S, Hong L, Dewerth A, Kormann MS, Salem AK, A comparative study of the bone regenerative effect of chemically modified RNA encoding BMP-2 or BMP-9, The AAPS journal 19(2) (2017) 438–446. [PubMed: 28074350]

[82]. Nakamura T, Shirakata Y, Shinohara Y, Miron RJ, Hasegawa-Nakamura K, Fujioka-Kobayashi M, Noguchi K, Comparison of the effects of recombinant human bone morphogenetic protein-2 and-9 on bone formation in rat calvarial critical-size defects, Clinical oral investigations 21(9) (2017) 2671–2679. [PubMed: 28197731]

[83]. Choi J-Y, Pratap J, Javed A, Zaidi SK, Xing L, Balint E, Dalamangas S, Boyce B, Van Wijnen AJ, Lian JB, Subnuclear targeting of Runx/Cbfa/AML factors is essential for tissue-specific differentiation during embryonic development, Proceedings of the National Academy of Sciences 98(15) (2001) 8650–8655.

[84]. Komori T, Yagi H, Nomura S, Yamaguchi A, Sasaki K, Deguchi K, Shimizu Y, Bronson R, Gao Y-H, Inada M, Targeted disruption of Cbfa1 results in a complete lack of bone formation owing to maturational arrest of osteoblasts, cell 89(5) (1997) 755–764. [PubMed: 9182763]

[85]. Kim I, Otto F, Zabel B, Mundlos S, Regulation of chondrocyte differentiation by Cbfa1, Mechanisms of development 80(2) (1999) 159–170. [PubMed: 10072783]

[86]. Inada M, Yasui T, Nomura S, Miyake S, Deguchi K, Himeno M, Sato M, Yamagiwa H, Kimura T, Yasui N, Maturational disturbance of chondrocytes in Cbfa1-deficient mice, Developmental dynamics: an official publication of the American Association of Anatomists 214(4) (1999) 279–290. [PubMed: 10213384]

[87]. Otto F, Thornell AP, Crompton T, Denzel A, Gilmour KC, Rosewell IR, Stamp GW, Beddington RS, Mundlos S, Olsen BR, Cbfa1, a candidate gene for cleidocranial dysplasia syndrome, is essential for osteoblast differentiation and bone development, Cell 89(5) (1997) 765–771. [PubMed: 9182764]

[88]. Papaioannou G, Mirzamohammadi F, Kobayashi T, MicroRNAs involved in bone formation, Cellular and molecular life sciences 71(24) (2014) 4747–4761. [PubMed: 25108446]

[89]. Li X, Guo L, Liu Y, Su Y, Xie Y, Du J, Zhou J, Ding G, Wang H, Bai Y, MicroRNA-21 promotes osteogenesis of bone marrow mesenchymal stem cells via the Smad7-Smad1/5/8-Runx2 pathway, Biochemical and biophysical research communications 493(2) (2017) 928–933. [PubMed: 28943430]

[90]. Song Q, Zhong L, Chen C, Tang Z, Liu H, Zhou Y, Tang M, Zhou L, Zuo G, Luo J, miR-21 synergizes with BMP9 in osteogenic differentiation by activating the BMP9/Smad signaling pathway in murine multilineage cells, International journal of molecular medicine 36(6) (2015) 1497–1506. [PubMed: 26460584]

[91]. Ji C, Liu X, Xu L, Yu T, Dong C, Luo J, RUNX1 plays an important role in mediating BMP9-lnduced osteogenic differentiation of mesenchymal stem cells line C3H10T1/2, murine multi-lineage cells lines C2C12 and MEFs, International journal of molecular sciences 18(7) (2017) 1348.

[92]. Wang Y, Feng Q, Ji C, Liu X, Li L, Luo J, RUNX3 plays an important role in mediating the BMP9-induced osteogenic differentiation of mesenchymal stem cells, International journal of molecular medicine 40(6) (2017) 1991–1999. [PubMed: 29039519]

[93]. Kreider BL, Benezra R, Rovera G, Kadesch T, Inhibition of myeloid differentiation by the helix-loop-helix protein Id, Science 255(5052) (1992) 1700–1702. [PubMed: 1372755]

[94]. Norton JD, Deed RW, Craggs G, Sablitzky F, Id helix—loop—helix proteins in cell growth and differentiation, Trends in cell biology 8(2) (1998) 58–65. [PubMed: 9695810]

[95]. Ruzinova MB, Benezra R, Id proteins in development, cell cycle and cancer, Trends in cell biology 13(8) (2003)410–418. [PubMed: 12888293]

[96]. Tang J, Gordon GM, Nickoloff BJ, Foreman KE, The helix–loop–helix protein id-1 delays onset of replicative senescence in human endothelial cells, Laboratory investigation 82(8) (2002) 1073–1079. [PubMed: 12177246]

[97]. Benezra R, Davis RL, Lockshon D, Turner DL, Weintraub H, The protein Id: a negative regulator of helix-loop-helix DNA binding proteins, Cell 61(1) (1990) 49–59. [PubMed: 2156629]

[98]. Massari ME, Murre C, Helix-loop-helix proteins: regulators of transcription in eucaryotic organisms, Molecular and cellular biology 20(2) (2000) 429–440. [PubMed: 10611221]

[99]. Murre C, Bain G, van Dijk MA, Engel I, Furnari BA, Massari ME, Matthews JR, Quong MW, Rivera RR, Stuiver MH, Structure and function of helix-loop-helix proteins, Biochimica et Biophysica Acta (BBA)-Gene Structure and Expression 1218(2) (1994) 129–135. [PubMed: 8018712]

[100]. Roberts EC, Deed RW, Inoue T, Norton JD, Sharrocks AD, Id helix-loop-helix proteins antagonize pax transcription factor activity by inhibiting DNA binding, Molecular and cellular biology 21(2) (2001) 524–533. [PubMed: 11134340]

[101]. Sun X-H, Copeland NG, Jenkins NA, Baltimore D, Id proteins Id1 and Id2 selectively inhibit DNA binding by one class of helix-loop-helix proteins, Molecular and cellular biology 11(11) (1991) 5603–5611. [PubMed: 1922066]

[102]. Peng Y, Kang Q, Cheng H, Li X, Sun MH, Jiang W, Luu HH, Park JY, Haydon RC, He TC, Transcriptional characterization of bone morphogenetic proteins (BMPs)-mediated osteogenic signaling, Journal of cellular biochemistry 90(6) (2003) 1149–1165. [PubMed: 14635189]

[103]. Lamplot JD, Qin J, Nan G, Wang J, Liu X, Yin L, Tomal J, Li R, Shui W, Zhang H, BMP9 signaling in stem cell differentiation and osteogenesis, American journal of stem cells 2(1) (2013) 1. [PubMed: 23671813]

[104]. Fisher A, Caudy M, The function of hairy-related bHLH repressor proteins in cell fate decisions, Bioessays 20(4) (1998) 298–306. [PubMed: 9619101]

[105]. Iso T, Sartorelli V, Poizat C, lezzi S, Wu H-Y, Chung G, Kedes L, Hamamori Y, HERP, a novel heterodimer partner of HES/E (spl) in Notch signaling, Molecular and cellular biology 21 (17) (2001) 6080–6089. [PubMed: 11486045]

[106]. Leimeister C, Externbrink A, Klamt B, Gessler M, Hey genes: a novel subfamily of hairy-and Enhancer of split related genes specifically expressed during mouse embryogenesis, Mechanisms of development 85(1-2) (1999) 173–177. [PubMed: 10415358]

[107]. Miao L, Li J, Li J, Tian X, Lu Y, Hu S, Shieh D, Kanai R, Zhou B.-y., Zhou B, Notch signaling regulates Hey2 expression in a spatiotemporal dependent manner during cardiac morphogenesis and trabecular specification, Scientific reports 8(1) (2018) 1–14. [PubMed: 29311619]

[108]. Blom IE, Goldschmeding R, Leask A, Gene regulation of connective tissue growth factor: new targets for antifibrotic therapy?, Matrix Biology 21(6) (2002) 473–482. [PubMed: 12392758]

[109]. Brigstock D, The CCN family: a new stimulus package, The Journal of endocrinology 178(2) (2003) 169–175. [PubMed: 12904165]

[110]. Lau LF, Lam SC-T, The CCN family of angiogenic regulators: the integrin connection, Experimental cell research 248(1) (1999) 44–57. [PubMed: 10094812]

[111]. Moussad EE-DA, Brigstock DR, Connective tissue growth factor: what's in a name?, Molecular genetics and metabolism 71(1-2) (2000) 276–292. [PubMed: 11001822]

[112]. Ivkovic S, Yoon BS, Popoff SN, Safadi FF, Libuda DE, Stephenson RC, Daluiski A, Lyons KM, Connective tissue growth factor coordinates chondrogenesis and angiogenesis during skeletal development, Development 130(12) (2003) 2779–2791. [PubMed: 12736220]

[113]. Lasky JA, Ortiz LA, Tonthat B, Hoyle GW, Corti M, Athas G, Lungarella G, Brody A, Friedman M, Connective tissue growth factor mRNA expression is upregulated in bleomycin-

induced lung fibrosis, American Journal of Physiology-Lung Cellular and Molecular Physiology 275(2) (1998) L365–L371.

[114]. Dou J, Wang T, Wang X, Zhang Y, Correlation between overexpression of connective tissue growth factor, tumor progression, and clinical prognosis in endometrial cancer patients, International Journal of Clinical and Experimental Pathology 11(4) (2018) 2100. [PubMed: 31938318]

[115]. Lambi AG, Pankratz TL, Mundy C, Gannon M, Barbe MF, Richtsmeier JT, Popoff SN, The Skeletal site-specific role of connective tissue growth factor in prenatal osteogenesis, Developmental Dynamics 241(12) (2012) 1944–1959. [PubMed: 23073844]

[116]. Tomita N, Hattori T, Itoh S, Aoyama E, Yao M, Yamashiro T, Takigawa M, Cartilage–specific over-expression of CCN family member 2/connective tissue growth factor (CCN2/CTGF) stimulates insulin-like growth factor expression and bone growth, PLoS One 8(3) (2013).

[117]. Jun Loh X, Lee T-C, Gene delivery by functional inorganic nanocarriers, Recent patents on DNA & gene sequences 6(2) (2012) 108–114. [PubMed: 22670611]

[118]. de Ilarduya CT, Sun Y, Düğüneş N, Gene delivery by lipoplexes and polyplexes, European journal of pharmaceutical sciences 40(3) (2010) 159–170. [PubMed: 20359532]

[119]. Medina-Kauwe L, Xie J, Hamm-Alvarez S, Intracellular trafficking of nonviral vectors, Gene therapy 12(24) (2005) 1734. [PubMed: 16079885]

[120]. Parker SE, Vahlsing HL, Serfilippi LM, Franklin CL, Doh SG, Gromkowski SH, Lew D, Manthorpe M, Norman J, Cancer gene therapy using plasmid DNA: safety evaluation in rodents and non-human primates, Human gene therapy 6(5) (1995) 575–590. [PubMed: 7578395]

[121]. Burke B, Sumner S, Maitland N, Lewis C, Macrophages in gene therapy: cellular delivery vehicles and in vivo targets, Journal of leukocyte biology 72(3) (2002) 417–428. [PubMed: 12223508]

[122]. Mumcuoglu D, Siverino C, Tabisz B, Kluijtmans B, Nickel J, How to use BMP-2 for clinical applications? A review on pros and cons of existing delivery strategies, (2017).

[123]. Madl CM, Mehta M, Duda GN, Heilshorn SC, Mooney DJ, Presentation of BMP-2 mimicking peptides in 3D hydrogels directs cell fate commitment in osteoblasts and mesenchymal stem cells, Biomacromolecules 15(2) (2014) 445–455. [PubMed: 24400664]

[124]. Bergeron E, Senta H, Mailloux A, Park H, Lord E, Faucheux N, Murine preosteoblast differentiation induced by a peptide derived from bone morphogenetic proteins-9, Tissue Engineering Part A 15(11) (2009) 3341–3349. [PubMed: 19388833]

[125]. Glynne Andrew J, Andrew SM, Freemont AJ, Marsh DR, Inflammatory cells in normal human fracture healing, Acta Orthopaedica Scandinavica 65(4) (1994) 462–466. [PubMed: 7976298]

[126]. Bergeron E, Leblanc E, Drevelle O, Giguere R, Beauvais S, Grenier G, Faucheux N, The evaluation of ectopic bone formation induced by delivery systems for bone morphogenetic protein-9 or its derived peptide, Tissue Engineering Part A 18(3-4) (2012) 342–352. [PubMed: 21902464]

[127]. Vhora I, Lalani R, Bhatt P, Patil S, Misra A, Lipid-nucleic acid nanoparticles of novel ionizable lipids for systemic BMP-9 gene delivery to bone-marrow mesenchymal stem cells for osteoinduction, International journal of pharmaceutics 563 (2019) 324–336. [PubMed: 30954673]

[128]. Tavassoli M, Structure and function of sinusoidal endothelium of bone marrow, Progress in clinical and biological research 59 (1981) 249–256.

[129]. Zhang R, Li X, Liu Y, Gao X, Zhu T, Lu L, Acceleration of bone regeneration in critical-size defect using BMP-9-loaded nHA/ColI/MWCNTs scaffolds seeded with bone marrow mesenchymal stem cells, BioMed research international 2019 (2019).

[130]. Li X, Zhang R, Li B, Tan X, Wang X, Biocompatible nHA/Col-BMP-9/GM Scaffold: Synthesis, Characterization, and Effects on Bone Marrow Mesenchymal Stem Cells, Journal of Hard Tissue Biology 28(2) (2019) 175–184.

[131]. Göz E, Karakeçili A, Effect of emulsification-diffusion parameters on the formation of poly (3-hydroxybutyrate-co-3-hydroxyvalerate) particles, Artificial cells, nanomedicine, and biotechnology 44(1) (2016) 226–234.

[132]. Saulacic N, Fujioka-Kobayashi M, Kobayashi E, Schaller B, Miron RJ, Guided bone regeneration with recombinant human bone morphogenetic protein 9 loaded on either deproteinized bovine bone mineral or a collagen barrier membrane, Clinical implant dentistry and related research 19(4) (2017) 600–607. [PubMed: 28466608]

[133]. Fujioka-Kobayashi M, Abd El Raouf M, Saulacic N, Kobayashi E, Zhang Y, Schaller B, Miron RJ, Superior bone-inducing potential of rhBMP9 compared to rhBMP2, Journal of Biomedical Materials Research Part A 106(6) (2018) 1561–1574. [PubMed: 29396910]

[134]. Fujioka-Kobayashi M, Schaller B, Saulacic N, Zhang Y, Miron RJ, Growth factor delivery of BMP9 using a novel natural bovine bone graft with integrated atelo-collagen type I: Biosynthesis, characterization, and cell behavior, Journal of biomedical materials research Part A 105(2) (2017) 408–418. [PubMed: 27699987]

[135]. Nakamura T, Shirakata Y, Shinohara Y, Miron RJ, Furue K, Noguchi K, Osteogenic potential of recombinant human bone morphogenetic protein-9/absorbable collagen sponge (rhBMP-9/ACS) in rat critical size calvarial defects, Clinical oral investigations 21(5) (2017) 1659–1665. [PubMed: 27726024]

[136]. Fujioka-Kobayashi M, Schaller B, Saulacic N, Pippenger BE, Zhang Y, Miron RJ, Absorbable collagen sponges loaded with recombinant bone morphogenetic protein 9 induces greater osteoblast differentiation when compared to bone morphogenetic protein 2, Clinical and experimental dental research 3(1) (2017) 32–40. [PubMed: 29744176]

[137]. Kobayashi M, Schaller B, Shirakata Y, Nakamura T, Noguchi K, Zhang Y, Miron RJ, Comparison of Two Porcine Collagen Membranes Combined with rhBMP-2 and rhBMP-9 on Osteoblast Behavior In Vitro, The International journal of oral & maxillofacial implants 32(4) (2017) e221–e230. [PubMed: 28708926]

[138]. Saulacic N, Schaller B, Muñoz F, Fujioka-Kobayashi M, Kobayashi E, Lang NP, Miron RJ, Recombinant human BMP9 (RhBMP9) in comparison with rhBMP2 for ridge augmentation following tooth extraction: An experimental study in the Beagle dog, Clinical oral implants research 29(10) (2018) 1050–1059. [PubMed: 30281171]

[139]. Gaihre B, Unagolla JM, Liu J, Ebraheim NA, Jayasuriya AC, Thermoresponsive Injectable Microparticle–Gel Composites with Recombinant BMP-9 and VEGF Enhance Bone Formation in Rats, ACS Biomaterials Science & Engineering 5(9) (2019) 4587–4600. [PubMed: 33448832]

[140]. Fujioka-Kobayashi M, Schaller B, Zhang Y, Kandalam U, Hernandez M, Miron RJ, Recombinant human bone morphogenetic protein (rhBMP) 9 induces osteoblast differentiation when combined with demineralized freeze-dried bone allografts (DFDBAs) or biphasic calcium phosphate (BCP), Clinical oral investigations 21(5) (2017) 1883–1893. [PubMed: 27771827]

[141]. Fujioka-Kobayashi M, Sawada K, Kobayashi E, Schaller B, Zhang Y, Miron RJ, Recombinant human bone morphogenetic protein 9 (rhBMP9) induced osteoblastic behavior on a collagen membrane compared with rhBMP2, Journal of periodontology 87(6) (2016) e101–e107. [PubMed: 26751345]

[142]. Fujioka-Kobayashi M, Mottini M, Kobayashi E, Zhang Y, Schaller B, Miron RJ, An in vitro study of fibrin sealant as a carrier system for recombinant human bone morphogenetic protein (rhBMP)–9 for bone tissue engineering, Journal of Cranio-Maxillofacial Surgery 45(1) (2017) 27–32. [PubMed: 27840120]

[143]. Fujioka-Kobayashi M, Schaller B, Kobayashi E, Hernandez M, Zhang Y, Miron RJ, Hyaluronic acid gel-based scaffolds as potential carrier for growth factors: An in vitro bioassay on its osteogenic potential, Journal of clinical medicine 5(12) (2016) 112.

[144]. Sheyn D, Kimelman-Bleich N, Pelled G, Zilberman Y, Gazit D, Gazit Z, Ultrasound-based nonviral gene delivery induces bone formation in vivo, Gene therapy 15(4) (2008) 257–266. [PubMed: 18033309]

[145]. Dijkmans P, Juffermans L, Musters R, van Wamel A, Ten Cate F, van Gilst W, Visser C, de Jong N, Kamp O, Microbubbles and ultrasound: from diagnosis to therapy, European Journal of Echocardiography 5(4) (2004) 245–246. [PubMed: 15219539]

[146]. Aslan H, Zilberman Y, Arbeli V, Sheyn D, Matan Y, Liebergall M, Li JZ, Helm GA, Gazit D, Gazit Z, Nucleofection-based ex vivo nonviral gene delivery to human stem cells as a platform for tissue regeneration, Tissue engineering 12(4) (2006) 877–889. [PubMed: 16674300]

[147]. Marquis M-E, Lord E, Bergeron E, Bourgoin L, Faucheux N, Short-term effects of adhesion peptides on the responses of preosteoblasts to pBMP-9, Biomaterials 29(8) (2008) 1005–1016. [PubMed: 18023475]

[148]. Park J, Ries J, Gelse K, Kloss F, Von Der Mark K, Wiltfang J, Neukam F, Schneider H, Bone regeneration in critical size defects by cell-mediated BMP-2 gene transfer: a comparison of adenoviral vectors and liposomes, Gene therapy 10(13) (2003) 1089–1098. [PubMed: 12808439]

[149]. Balmayor ER, van Griensven M, Gene therapy for bone engineering, Frontiers in bioengineering and biotechnology 3 (2015) 9. [PubMed: 25699253]

[150]. Zhang Y, Fan W, Nothdurft L, Wu C, Zhou Y, Crawford R, Xiao Y, In vitro and in vivo evaluation of adenovirus combined silk fibroin scaffolds for bone morphogenetic protein-7 gene delivery, Tissue Engineering Part C: Methods 17(8) (2011) 789–797. [PubMed: 21506685]

[151]. Evans CH, Gene delivery to bone, Advanced drug delivery reviews 64(12) (2012) 1331–1340. [PubMed: 22480730]

[152]. Ye J, Wang J, Zhu Y, Wei Q, Wang X, Yang J, Tang S, Liu H, Fan J, Zhang F, A thermoresponsive polydiolcitrate-gelatin scaffold and delivery system mediates effective bone formation from BMP9-transduced mesenchymal stem cells, Biomedical Materials 11(2) (2016) 025021. [PubMed: 27097687]

[153]. Dumanian ZP, Tollemar V, Ye J, Lu M, Zhu Y, Liao J, Ameer GA, He T-C, Reid RR, Repair of critical sized cranial defects with BMP9-transduced calvarial cells delivered in a thermoresponsive scaffold, PloS one 12(3) (2017).

[154]. Lee CS, Bishop ES, Dumanian Z, Zhao C, Song D, Zhang F, Zhu Y, Ameer GA, He T-C, Reid RR, Bone morphogenetic protein-9–stimulated adipocyte-derived mesenchymal progenitors entrapped in a thermoresponsive nanocomposite scaffold facilitate cranial defect repair, Journal of Craniofacial Surgery 30(6) (2019) 1915–1919.

[155]. Zou Y, Qazvini NT, Zane K, Sadati M, Wei Q, Liao J, Fan J, Song D, Liu J, Ma C, Gelatin-Derived Graphene–Silicate Hybrid Materials Are Biocompatible and Synergistically Promote BMP9-Induced Osteogenic Differentiation of Mesenchymal Stem Cells, ACS applied materials & interfaces 9(19) (2017) 15922–15932. [PubMed: 28406027]

[156]. Nie L, Yang X, Duan L, Huang E, Pengfei Z, Luo W, Zhang Y, Zeng X, Qiu Y, Cai T, The healing of alveolar bone defects with novel bio-implants composed of Ad-BMP9-transfected rDFCs and CHA scaffolds, Scientific reports 7(1) (2017) 1–11. [PubMed: 28127051]

[157]. Fu T, Liang P, Song J, Wang J, Zhou P, Tang Y, Li J, Huang E, Matrigel scaffolding enhances BMP9-induced bone formation in dental follicle stem/precursor cells, International journal of medical sciences 16(4) (2019) 567. [PubMed: 31171908]

Highlights

- BMP-9 plays a major role in osteogenic differentiation of stem cells.
- Crucial advantage of BMP-9 over other BMPs is its resistance to noggin inhibition.
- Synergism of biomaterial matrix and BMP-9 plays role in optimal delivery.
- Non-viral vector delivery of BMP-9 is safer than its viral vector counterpart.
- BMP-9 at low dosage using non-viral polymeric vector displays promising results.

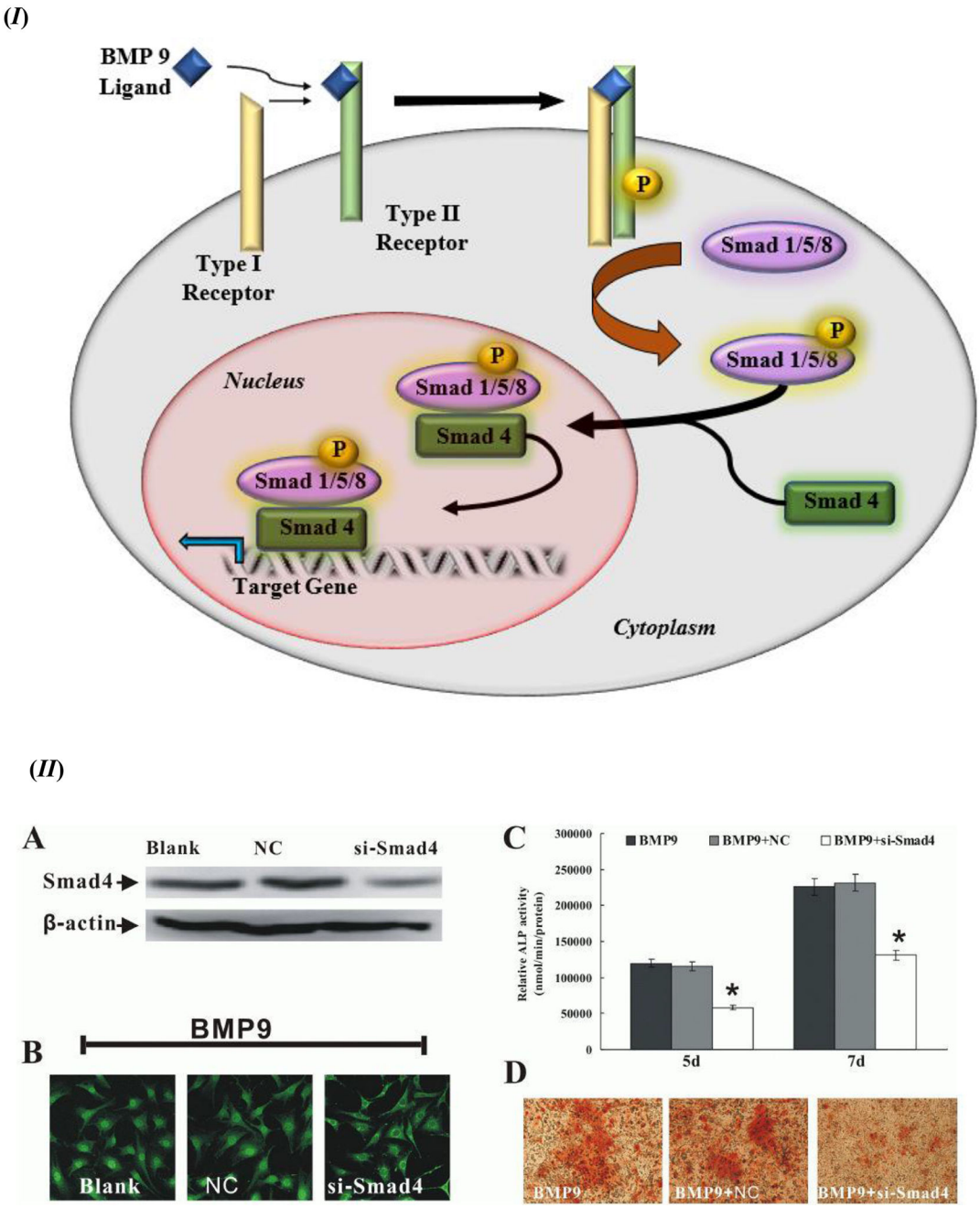

Figure 1.

(*I*) Schematic representation of a stem cell with the Smad signaling pathway activated by the binding of the BMP-9 ligand with the specific BMP-9 receptor. Smad 4 plays a critical role in nuclear translocation of the Smad complex that binds to its DNA promoter element to express the target gene. (*II*) Smads (1/5/8 as well as 4) are a quintessential component of the BMP-9 osteogenic differentiation cell signaling cascade. The cells used in this case were C3H10T1/2 mesenchymal stem cells: (A) Smad 4 knockdown (si-Smad4) was confirmed using Western Blot (β-actin used as a loading control); (B) C3H10T1/2 mesenchymal stem cells were transfected with Adenoviral-si-Smad 4 first and then exposed to BMP-9

conditioned medium. Immunochemistry staining after 4 h of BMP-9 exposure shows Smad 1/5/8 nuclear translocation (x40 magnification); (C) ALP activity detection at day 5 and day 7 after BMP-9 stimulation (after Smad 4 knockdown was carried out). * p value < 0.05 vs Negative Control (NC). Data collected from triplicates (mean ± SD); (D) Biomineralization, or calcium deposition after day 21 post-BMP-9 stimulation and Smad 4 knockdown (x100 magnification). Figure 1. (*II*) reprinted from [73] from BMB Reports; Open Access License (http://www.bmbreports.org/).

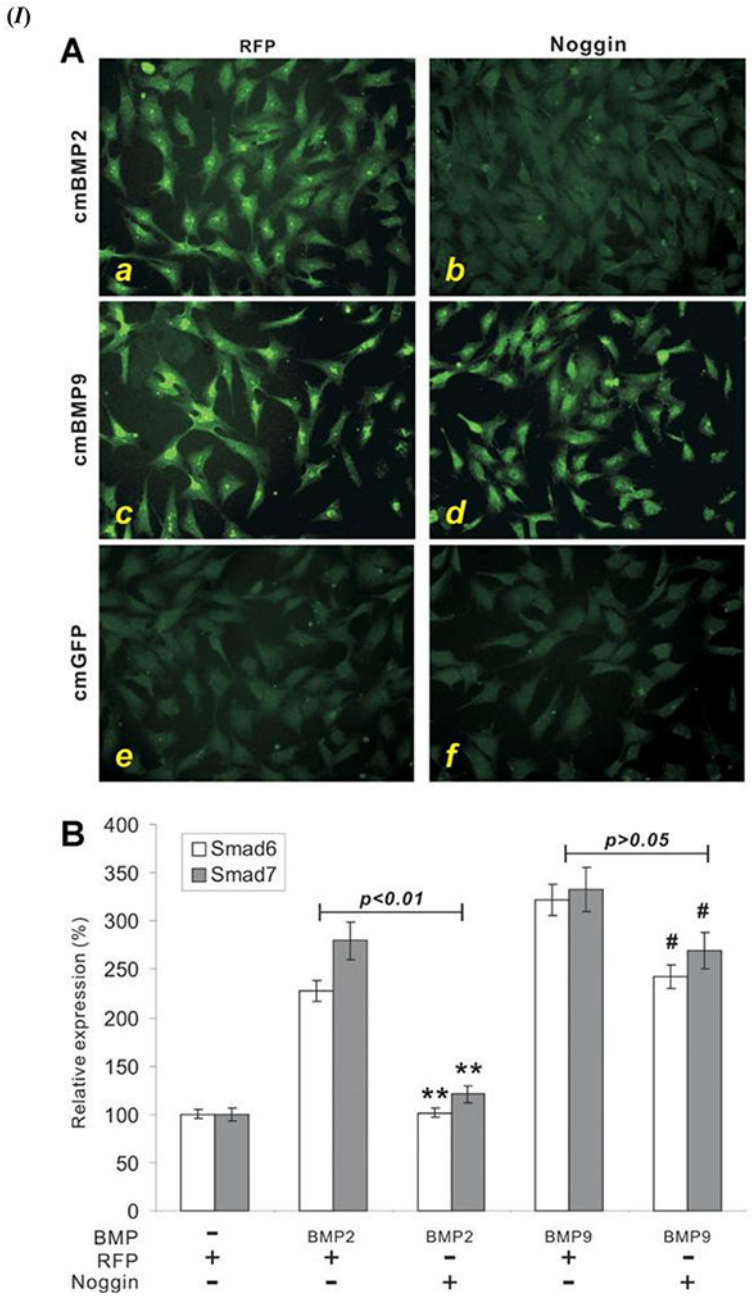

(*II*)

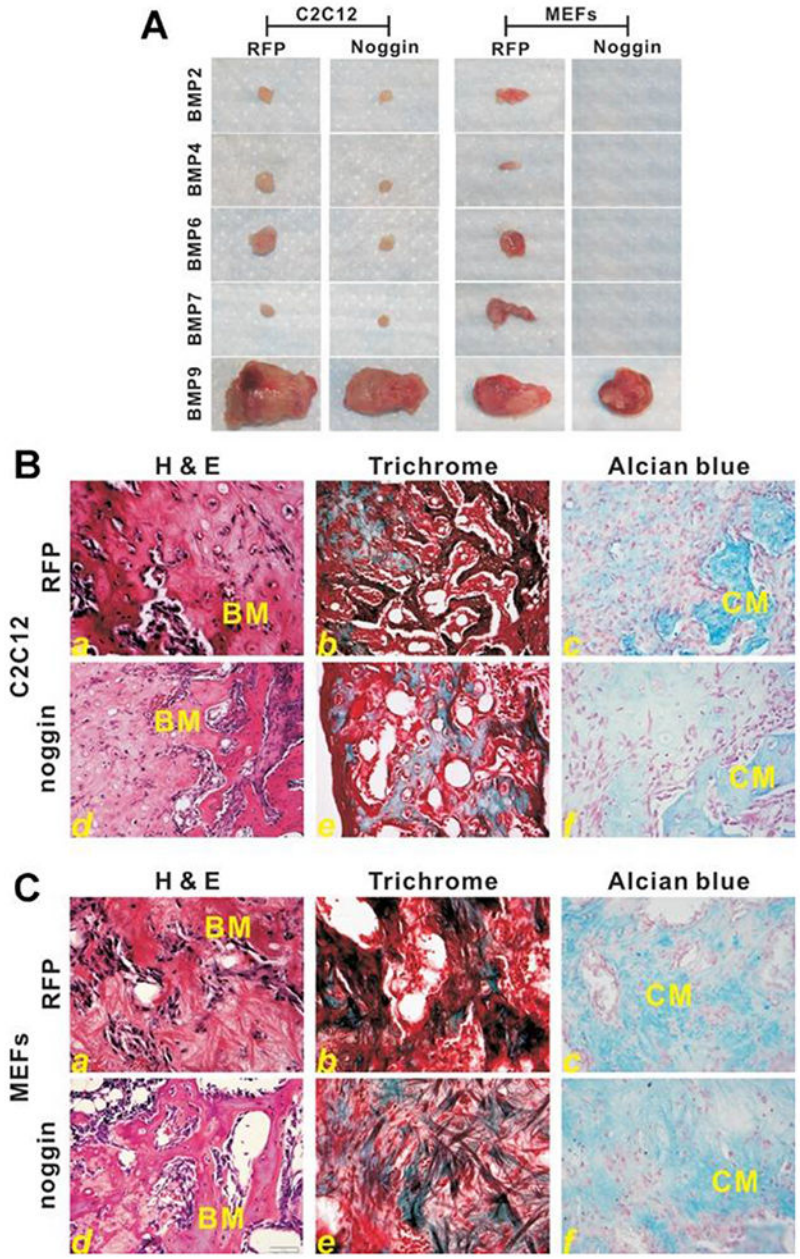

Figure 2.

(*I*) BMP-9 triggered Smad signaling pathway is resistant to Noggin in Mesenchymal Stem Cells (MSCs). (A) Noggin inhibition of Smad activation in BMP 2. Adenoviral (Ad) expressing Noggin (Ad-Noggin) or Ad-Red Fluorescent Protein (RFP) were exposed to the C2C12 cells; cells were cultured overnight in Fetal Bovine Serum (1%) overnight. Three different media were categorized as cmBMP2 (a, b), cmBMP9 (c, d), and cmGFP (Green Fluorescent Protein) (e, f) in which the infected cells were treated for 2 h. Immunofluorescence staining using anti-Smad 1/5/8 antibody (from Santa Cruz Biotechnology); Negative control used for the experiment was either control IgG or absence

of primary antibody staining. (B) Smad 6/7, induced by the BMP-9 signaling cascade, is expressed in the presence of Noggin; proves the resistance of BMP-9 towards Noggin inhibition. Sub confluent C2C12 cells were used for this experiment; these cells were infected with Ad-BMP 2/9 and Ad-Noggin or Ad-RFP for 30 h. Reverse transcription-polymerase chain reaction (RT-PCR) analysis using mouse Smad 6 and Smad 7 primers was done on the isolated total RNA from the infected cells. Normalization control used was GAPDH with triplicates done for all assays. Noggin vs. RFP expression (Smad 5 and Smad 7) ** p value < 0.01, # p value < 0.05. (*II*) Noggin resistance is displayed by BMP-9 during ectopic bone formation. (A). Ectopic bone masses formed with two different cell lines, C2C12 and mouse embryonic fibroblasts (MEFs), infected with the Ad-BMP-9 and then injected subcutaneously injected into athymic mice with and without Noggin. These samples were from 4 weeks post-injection. (B) Histological evaluation of the samples harvested from Ad-BMP-9 infected C2C12 cell injection site; (a) H& E staining, (b) Trichrome staining, and (c) Alcian blue staining. (C) Histological evaluation of the samples harvested from Ad-BMP-9 infected MEFs cell injection site; (a) H& E staining, (b) Trichrome staining, and (c) Alcian blue staining. X200 magnification. BM – Bone matrix; CM – chondroid or cartilage matrix. Figures 2. (*I*) and (*II*) reprinted from [45] with permission from John Wiley and Sons.

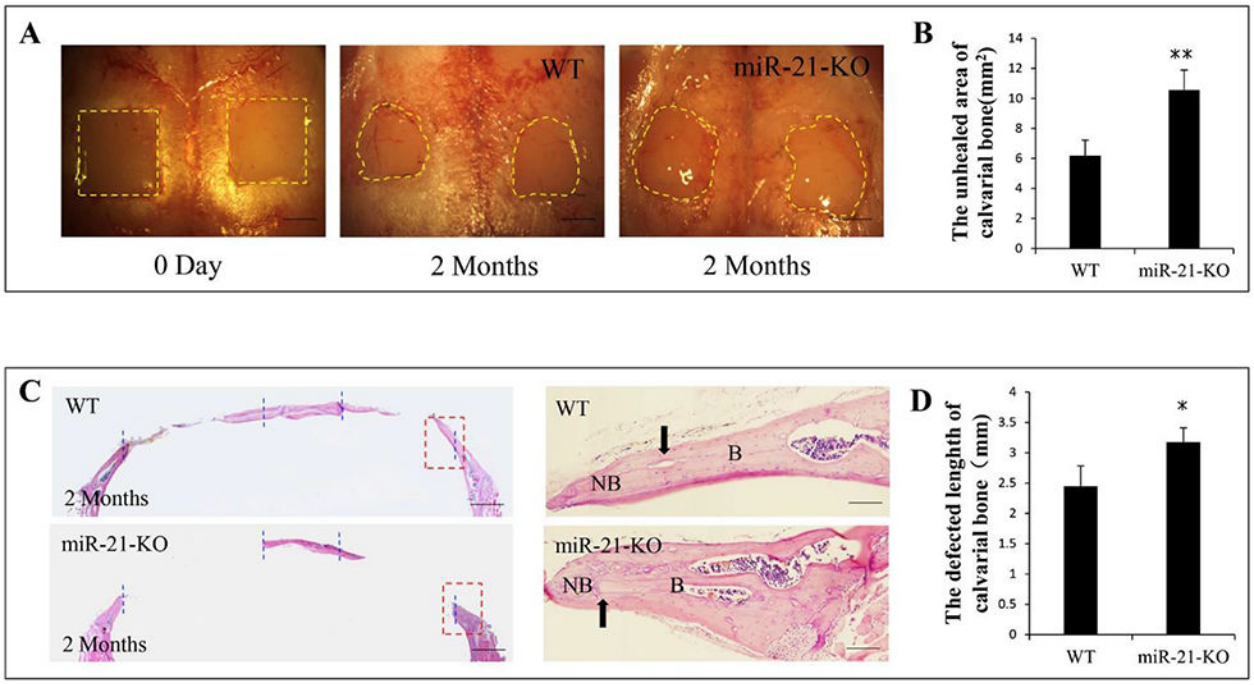

Figure 3.

Inadequate bone formation was observed with MiR-21 deficiency in Calvarial bone defects. (A) Calvarial bone defects (4 mm by 4 mm each) for wild-type (WT) and MiR-21 knockout (miR-21-KO) mice with respect to zero time and 2 months. (B) After 2 months of surgery, the MiR-21 knockout samples showed a significantly smaller amount of bone formation in those calvarial defects; the comparison was done at a p value < 0.01. (C) Histology analysis displayed significant bone healing in WT in comparison to knockout mice; B – host bone, NB – new bone. (D) At a p value < 0.05, the comparison between the two groups exhibited a significant difference in defect length; an increase in the defect length infers a slower new bone formation for closing the defect. All data are shown as means ± SD; * p value < 0.05 and ** p value < 0.01; all experiments done with triplicates. Figure 3 reprinted from [89] with permission from Elsevier. Copyright © 2017 Elsevier Inc.

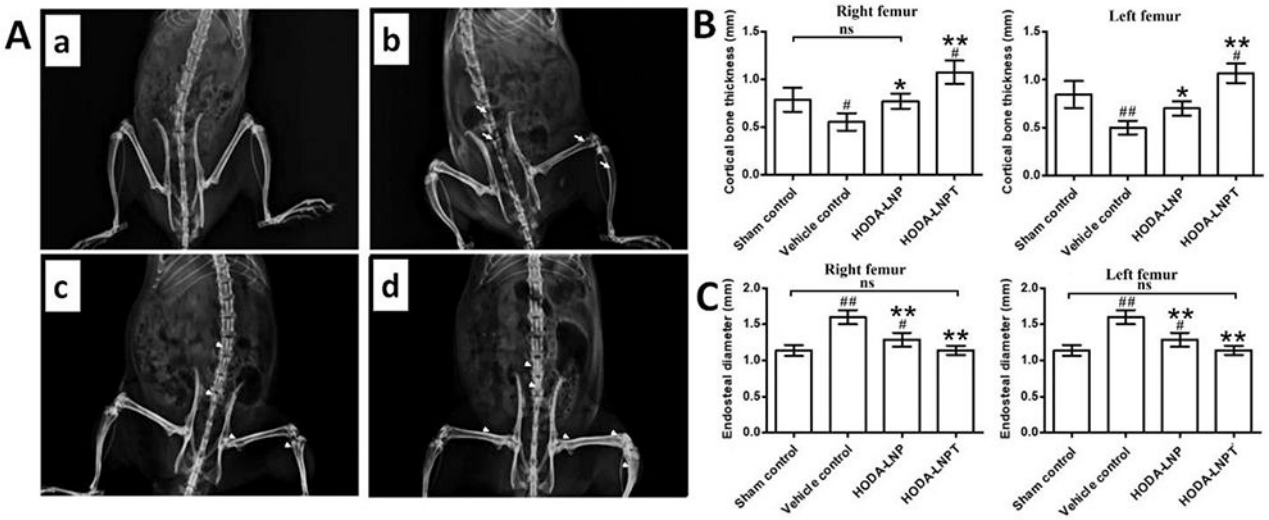

Figure 4.

OVX rat model with induced osteoporosis response to *in vivo* activity of the LNP delivery system. (A) X-ray radiographs showing (a) sham control rat, (b) OVX rat as vehicle control, (c) OVX rat with BMP-9 containing LNP, and (d) OVX rat with BMP-9 peptide containing LNP. (B) Left and right femur bone quantitative data for cortical thickness among separate groups. (C) Endosteal diameter quantitative analysis results for left and right femur bones among separate groups. * p value ≤ 0.05 and ** p value ≤ 0.01 in comparison with vehicle control group; # p value ≤ 0.05 and ## p value ≤ 0.01 in comparison with vehicle control group; ns – not statistically significant difference. Figure 4 reprinted from [127] with permission from Elsevier. Copyright © 2019 Elsevier B.V.

(*I*)

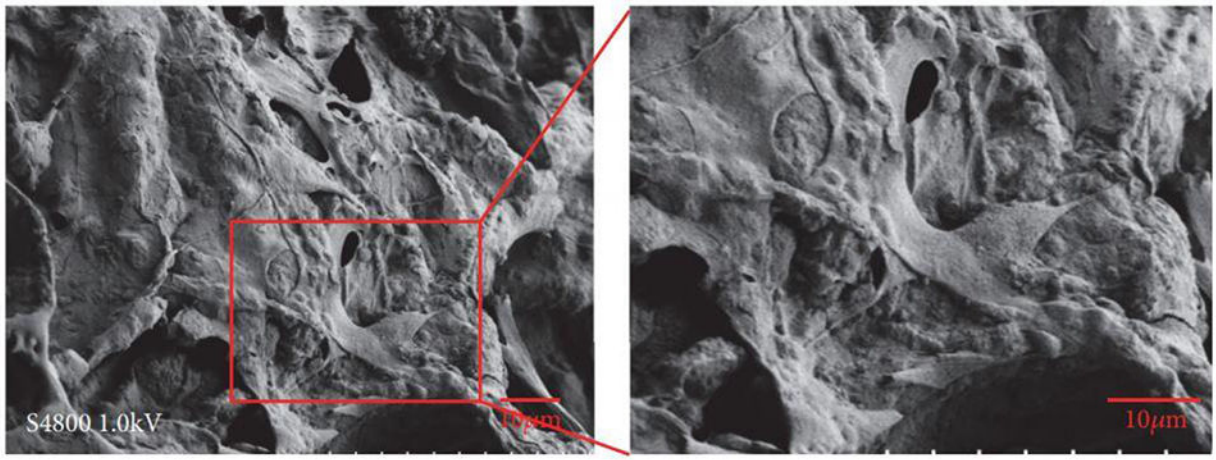

(*II*)

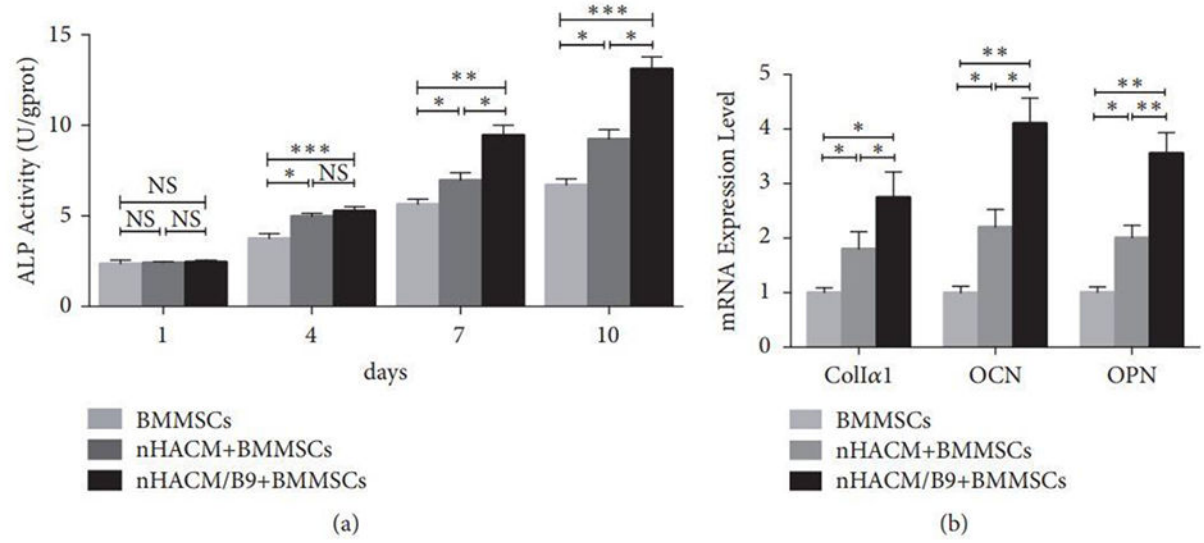

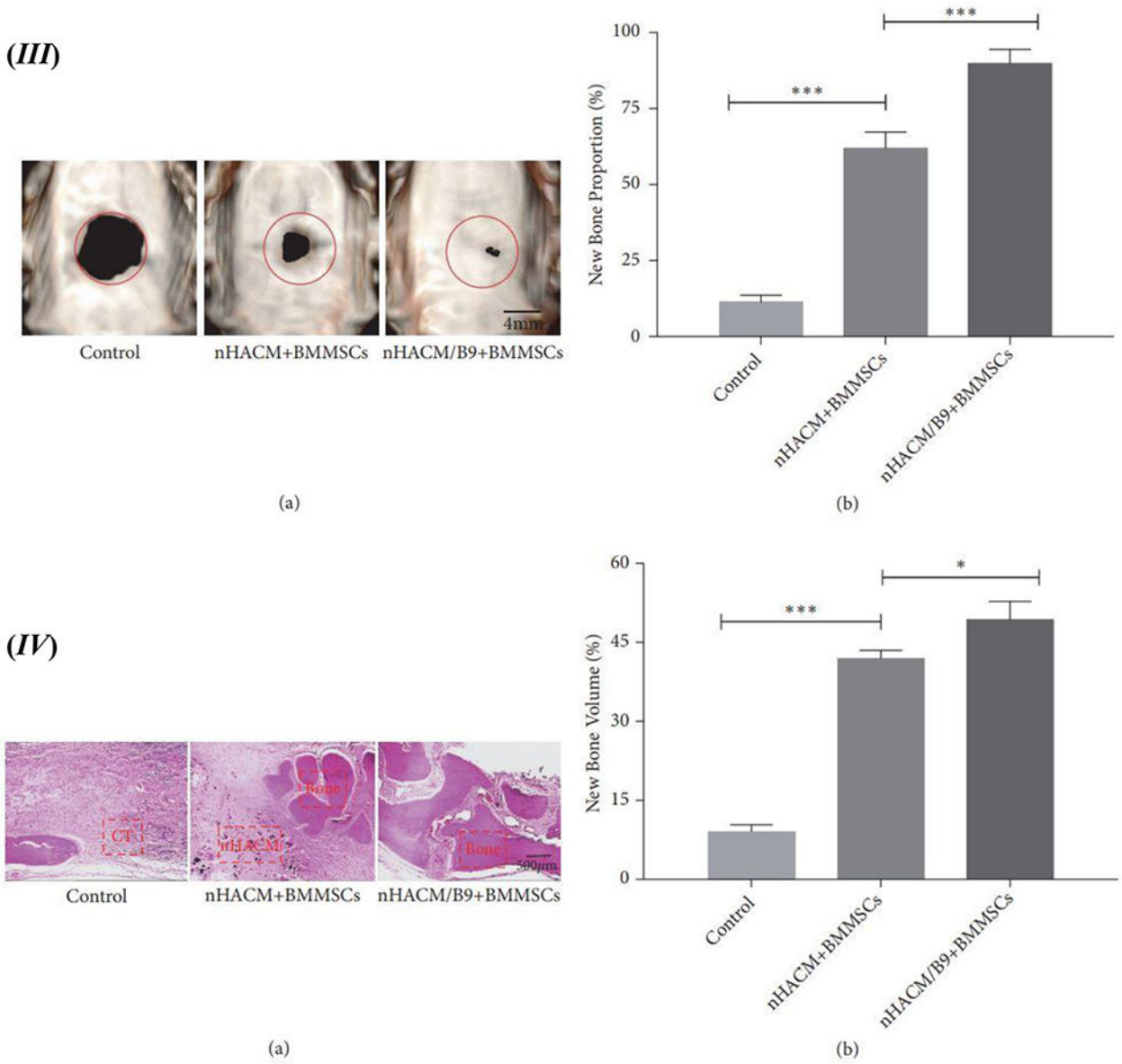

Figure 5.

(*I*) Bone marrow mesenchymal stem cells (BMMSCs) seeded on the nHACM/BMP-9 scaffolds; BMP-9 has been denoted as B9. Electron microscopy micrograph for cell attachment after 72 h of incubation. A randomized distribution pattern is observed for the cell on the BMP-9 containing scaffold. Scale = 10 μm. (*II*) Osteogenic differentiation upregulation is facilitated by BMP-9 containing scaffolds. (a) ALP activity reports significant enhancement with BMP-9 (denoted as B9) presence on the scaffolds after 4 days of culture with BMMSCs, as compared to controls cell only and scaffold without BMP-9; Days 7 and 10 show further significant enhancement in ALP activity. (b) qPCR evaluation of mRNA expressions that are a quintessential part of osteogenic differentiation – Col1α1, OCN, and OPN while culturing BMMSCs on scaffolds. BMP-9 (denoted as B9) containing scaffold group significantly showed the highest expression of these osteogenic marker genes. (*III*) Radiographs from *in vivo* samples after 12 weeks of bone healing post-surgery. (a)

Micro-CT images showing significantly larger bone formation area for the BMP-9 (denoted as B9) containing nHACM scaffold group, as compared to the control BMMSCs and scaffold only (nHACM + BMMSCs); red circles mark the site of the original bone defect. (b) Significantly higher bone proportion formation was observed with BMP-9 (denoted as B9) containing nHACM scaffold group. (*IV*) Histology analysis of 12-week old samples post-surgery. (a) New bone formation observed in scaffold containing groups, as compared to the control group. Remaining fragments of biodegradation of nHACM were also seen. (b) Bone volume quantification for the new bone formation process revealed significantly higher bone defect healing for the scaffold containing groups, and the BMP-9 (denoted as B9) + nHACM group significantly as the highest bone repair potential under those experimental conditions. The control group was reported to be filled with connective tissue. All data represented as Means ± SD; experiments were done in triplicates; * p value < 0.05, ** p value < 0.01, and *** p value < 0.001. Figure 5. (*I*), (*II*), (*III*), and (*IV*) reprinted (adapted) from [129]. Open Access Permission from Hindawi (https://www.hindawi.com/). Copyright © 2019 Ran Zhang et al.

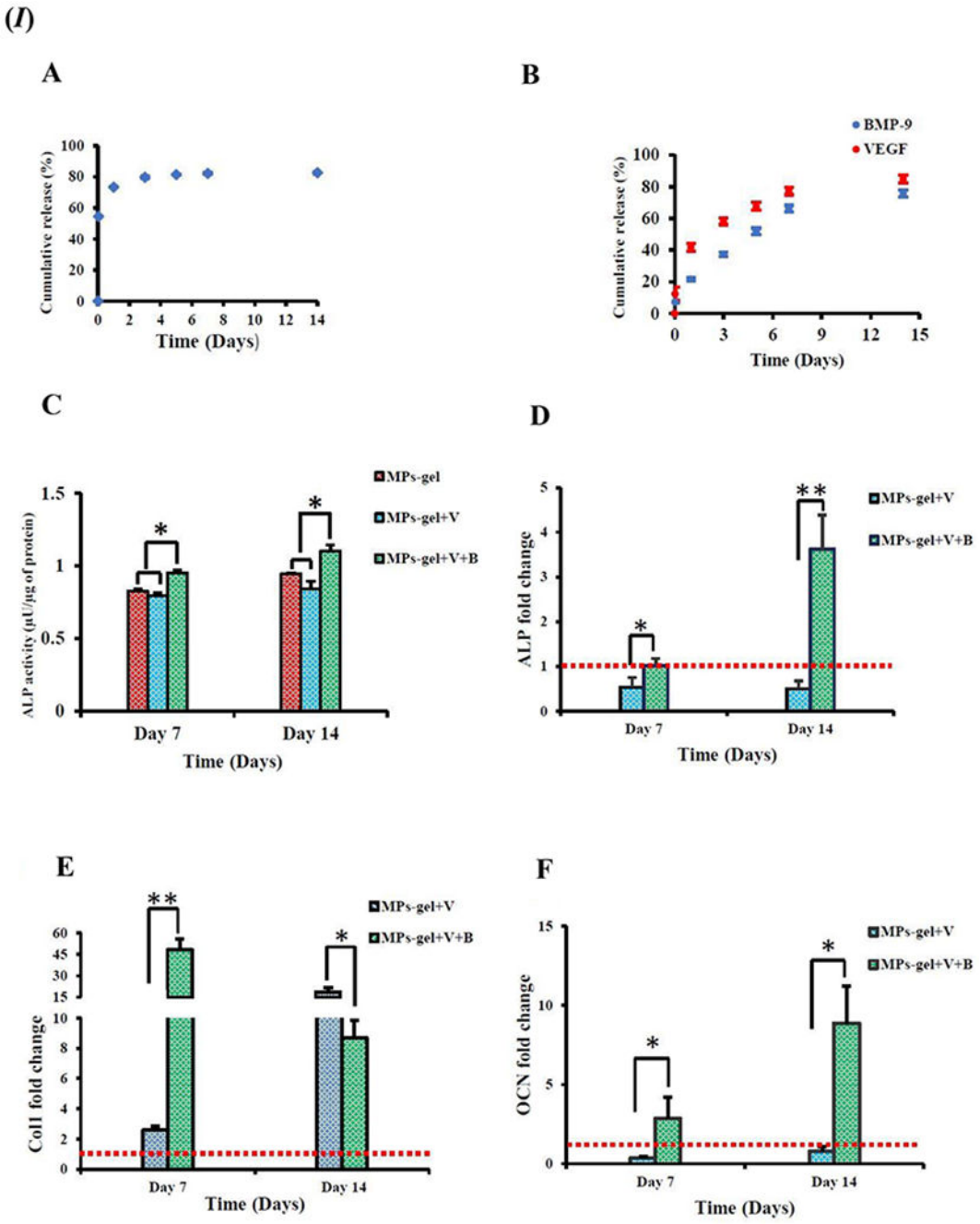

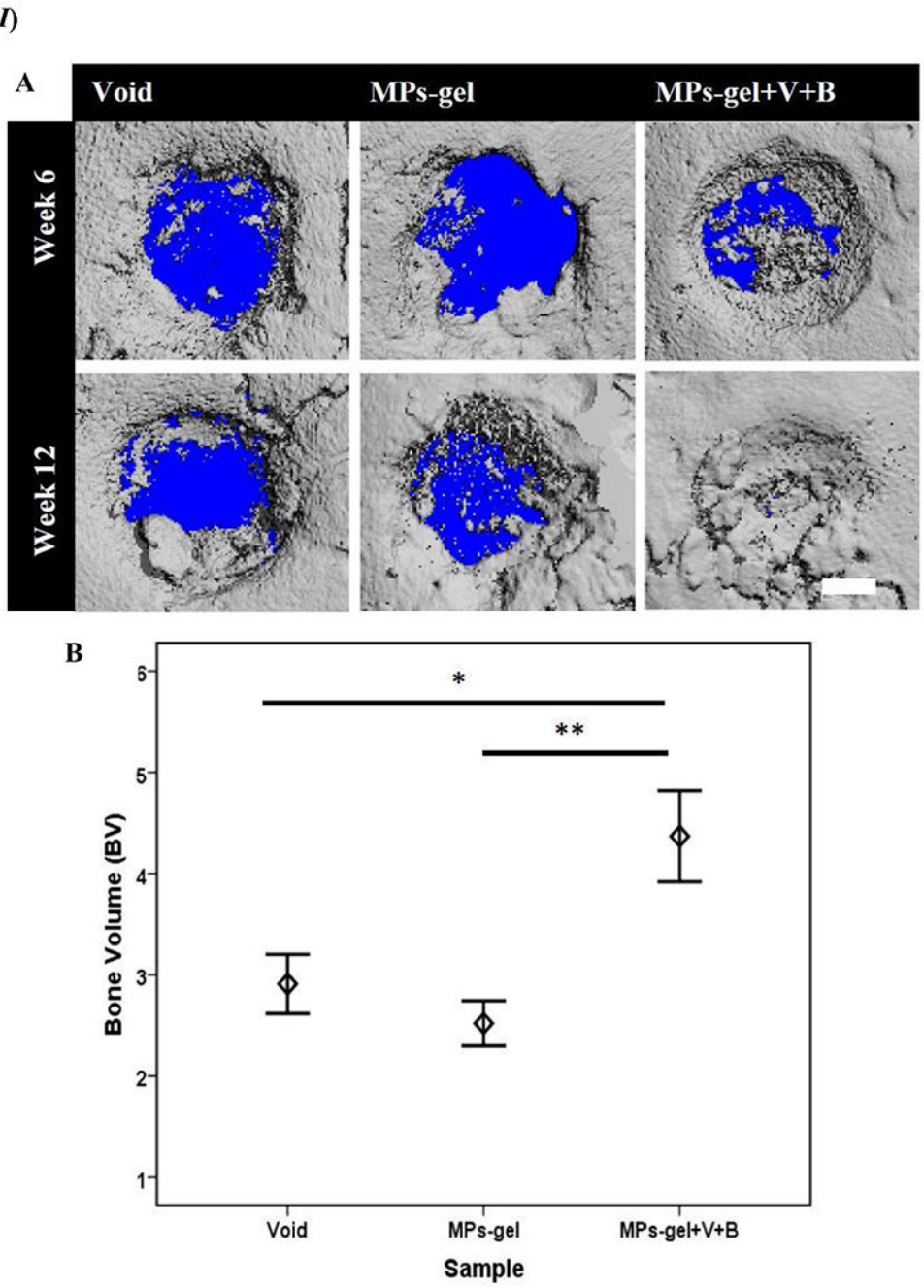

Figure 6.

(*I*) Osteogenic differentiation of hMSCs. (A) Cumulative release profile of BMP-9 from the BMP-9 coated microparticles; initial burst release evident. (B) Sustained release scenario for BMP-9 while the gel acts as a reservoir of initial burst release of BMP-9 from microparticles. VEGF added to the gel blend also follows a sustained release profile, however, at a faster rate than BMP-9. (C) ALP activity of hMSCs seeded with gel scaffold with or without BMP-9 presence (B – BMP-9, V – VEGF, MPs – Microparticles, Gel – Gel blend only). (D, E, F) RT-PCR quantification of osteogenic markers (number of folds change). The red dotted line represents the reference level of MPs + Gel as control. (*II*)

Calvarial bone defect (of size 3.5 mm in diameter) healing in a rat model. (A) Micro-CT images of bone healing in the bone defects.3D reconstruction of bone defect sites at 6 weeks and 12 weeks. (B) Quantitative analysis for bone volume in the defect site. * p value < 0.05 and ** p value < 0.001. Figure 6. (*I*) and (*II*) reprinted (adapted) with permission from [139]. Modifications: Changed numbering scheme to the uppercase alphabet in Figure 6. (*I*) and (*II*). Copyright © 2019 American Chemical Society.

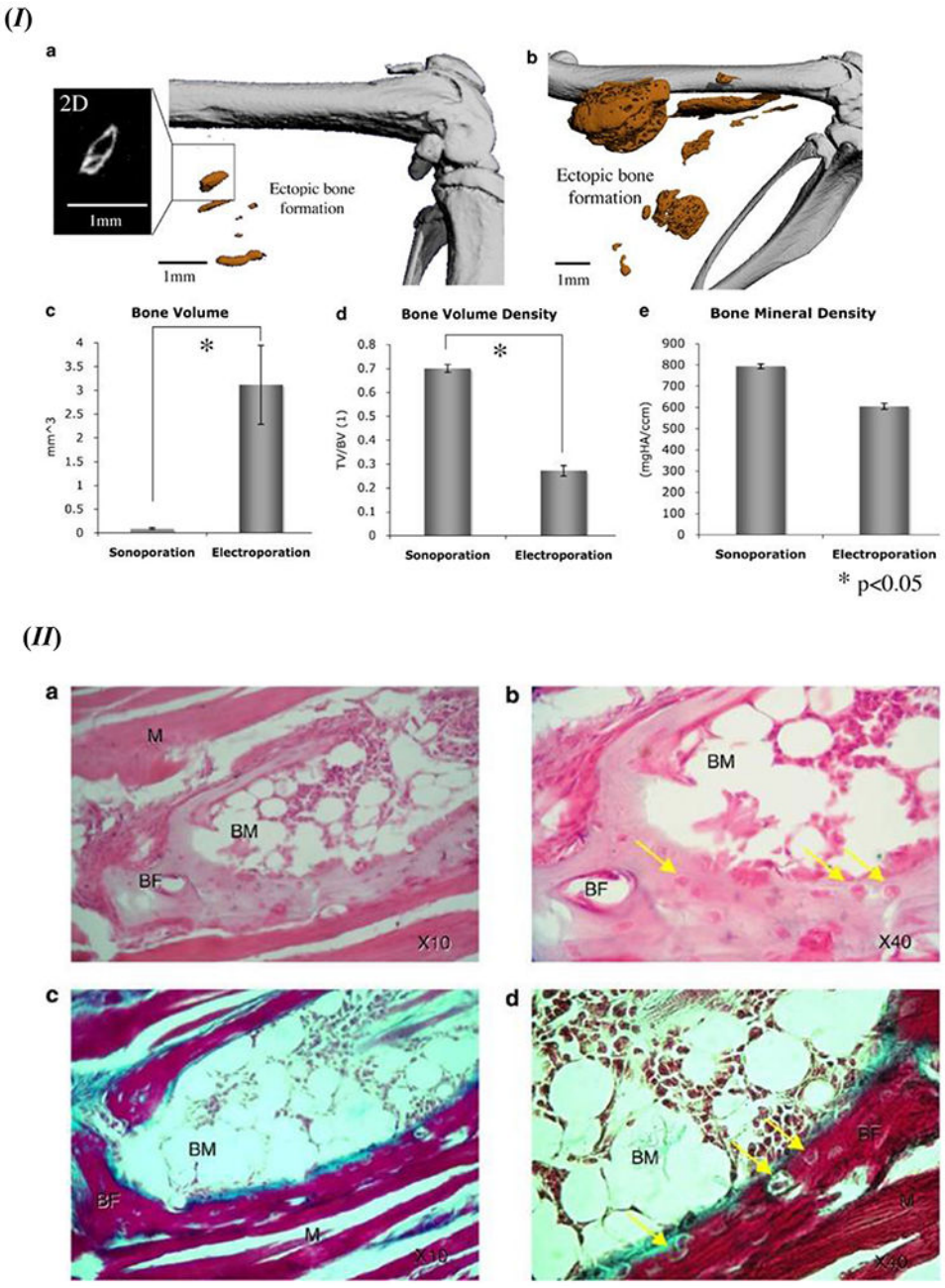

Figure 7.

(*I*) Recombinant BMP-9 induced ectopic bone formation using the sonoporation or electroporation method. Micro-CT images in high resolution for the detection of ectopic bone formation in thigh muscles of the mouse model using (a) sonoporation and (b) electroporation; 3D representation of the ectopic bone formation induced *in vivo*. 2D image of representative ectopic bone formation showed an enlarged format on the left of (a). Ectopic bone formation quantitative analysis of bone volume (c), volume density of the formed bone (d), and mineral density of the ectopic bone segment (e). Standard error bars shown for n=9. (*II*) Histology evaluation of the ectopic bone formation induced by rhBMP-9 in the *in vivo* mouse model. After 6 weeks post-sonoporation (a and b) H&E staining results

and (c and d) Masson trichrome staining data; BF – bone formation, BM – bone marrow, M – skeletal muscle; osteocytes are identified with the yellow arrows. Figure 7. (*I*) and (*II*) - Reprinted by permission from Springer Nature: Gene Therapy [144], D. Sheyn, N. Kimelman-Bleich, G. Pelled, Y. Zilberman, D. Gazit, Z. Gazit, Ultrasound-based nonviral gene delivery induces bone formation in vivo. Copyright © 2007, Springer Nature.

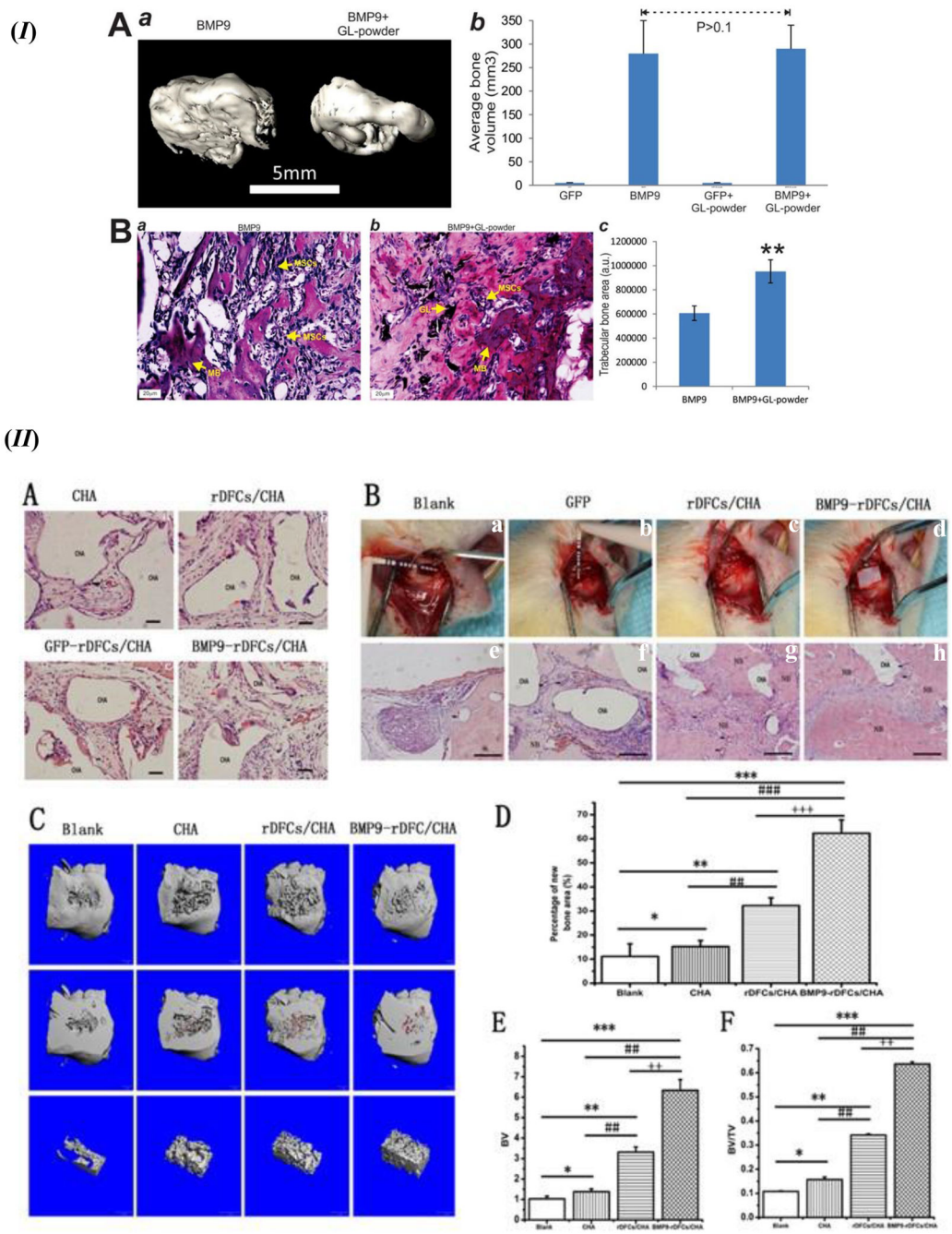

Figure 8.

(*I*) Ectopic bone formation induced by BMP-9 containing GL powder. (A) Micro-CT images of the ectopic bone formation. (a) 3D reconstruction of the harvested ectopic bone samples with iMEFs infected with BMP-9 and BMP-9 + GL powder. Ad-GFP control infected iMEFs and iMEFs + GL powder group was reported to have no significant ectopic bone formation induced. (b) Quantification of mean bone volume of the sample groups using Amira data visualization and processing program. (B) Histology analysis of extracted ectopic bone masses; (a and b) H & E staining. (c) Trabecular bone area formation quantification using ImageJ image processing program. GL – GL powder, MP – mineralized

bone matrix, MSCs – stem cells left undifferentiated. ** p value <0.05 in comparison with BMP-9 only group. Figure 8. (*I*) reprinted (adapted) with permission from [155]. Copyright © 2017, American Chemical Society. (*II*) In vivo analysis of new bone formation. (A) Ectopic bone formation analysis using H & E staining. (B) Alveolar bone defect implantation surgical procedure (a, b, c, and d). H & E staining showing new bone formation from the alveolar bone defects (e, f, g, h); Scale = 5 μm; CHA – Coralline hydroxyapatite scaffold, NB – new bone, red arrow denotes macrophages, black arrow denotes blood vessels. (C) Micro-CT and 3D reconstructed representative images of the alveolar defects with new bone formation for each experiment group. (D) New bone formation comparison by area. (E) Comparison of new bone volume. (F) Ratio of new bone formation bone volume (BV) over total bone volume (TV): BV/TV. * p value < 0.05, ** p value < 0.01, *** p value < 0.001 in comparison to the blank group, # p value < 0.05, ## p value < 0.01, ### p value < 0.001 in comparison to the CHA group, ++ p value < 0.01, +++ p value < 0.001 compared with rDFCs/CHA group. Modifications: Added alphabetical numbering in 8 (*II* B). *Figure* 8. (*II*) - Reprinted from [156] by permission from Springer Nature (Open Access): Copyright © 2017, Springer Nature.

Table 1.

Advantages of BMP-9 over BMP-2 in bone tissue regeneration.

Property	BMP-2	BMP-9	Delivery System	Advantage of BMP-9 over BMP-2	Reference
Alkaline Phosphatase (ALP) Activity	• Required lowest viral concentration of 2×10^4 PFU for ALP activity; 45×10^{-12} U/well (at a viral concentration of 2×10^5 PFU /well). • ALP gene expression less than 1.5.	• Required lowest viral concentration of 2×10^3 PFU for ALP activity; 4890×10^{-12} U/well (at a viral concentration of 2×10^5 PFU/well). • ALP gene expression close to 2.0.	• Adenovirus infected C2C12 Cells. • Chemically modified RNA encoding BMP loaded on collagen scaffold treated on Bone Marrow Stem cells.	• Reduced viral concentration required for inducing ALP activity. • Significantly higher ALP activity at a constant viral concentration. • Significantly higher ALP activity with BMP-9 transfected cells.	[80, 81]
Expression of BMP in Infected Cells	• 620 ng/ml (infected with 2×10^6 PFU viral concentration).	• 805 ng/ml (infected with 2×10^6 PFU viral concentration).	• Adenovirus infected C2C12 Cells.	• Higher expression of BMP from cells at constant viral concentration.	[80]
Osteogenic Potential	• Bone volume of 0.37±0.03 (at a mean viral concentration of 10^7 PFU) & 0.17±0.04 (at a mean viral concentration of 2×10^6 PFU); more chondrocytes were observed through histology studies. • Normalized calcium ion deposition (using atomic absorption spectrometer) close to 2 nmol/ml; bone connectivity density (at 50 μg BMP concentration per scaffold) was 14 fold more than control; 37.7% ± 4.7 bone regenerated area via histology analysis. • 8 weeks post *in vivo* surgery showed large fatty marrow spaces in the new bone.	• Bone volume of 0.63±0.07 (at a mean viral concentration of 10^7 PFU) & 0.35±0.06 (at a mean viral concentration of 2×10^6 PFU); more osteoblast traffic was observed through histology studies. • Normalized calcium ion deposition (using atomic absorption spectrometer) close to 3 nmol/ml; bone connectivity density (at 50 μg BMP concentration per scaffold) was 23 fold more than control; 18.6% ± 4.0 bone regenerated area via histology analysis. • 8 weeks post *in vivo* surgery showed denser new bone with less fatty marrow spaces with more osteocytes.	• BMP adenoviruses induced ectopic bone generation in athymic nude mice at 30 days. • Chemically modified RNA encoding BMP loaded on collagen scaffold treated on bone marrow Stem cells; critical-sized (5 mm diameter) calvarial defects in a rat model. • Recombinant BMP loaded on absorbable collagen sponges implanted on 5 mm calvarial defect on 17 weeks old male Wistar rats.	• Significantly increased bone volume at both doses of viral carrier mediated respective BMP treatment; Masson's trichrome staining shows increased collagen induction. • Alizarin red staining and atomic absorption spectrometry reveal significantly higher calcium deposition; 2 fold increase in bone connectivity density. • Morphology of the new bone formed was closer to natural bone post 8 weeks surgery.	[80-82]

Table 2.

Biomaterials in recent use for non-viral delivery systems and their benefits.

Biomaterial(s) for Matrix	Delivery System/Model	Key Features	Advantages	References
Chitosan, Col1agen	Peptide derived BMP-9 (pBMP-9)	• Derived from recombinant BMP-9 (rhBMP-9). • Higher concentrations (400 ng/ml) inhibits murine preosteoblasts cell proliferation. • Low concentration (less than 100 ng/ml) highlighted the promising results in comparison to rhBMP-9 and rhBMP-2. • Chitosan as a carrier for pBMP-9 is more effective over type I collagen constructs in terms of release kinetics of pBMP-9 and ectopic bone formation. • Lipid -nucleic acid nanoparticles (LNPs) may be loaded with pBMP-9 for stabilizing bone remodeling during osteoporosis.	• Viable cost-effective alternative to rhBMP-9. • Resistance to noggin inhibition mimicked by pBMP-9 while driving Smad 1/5/8 phosphorylation. • ALP activity reached a steady-state of around 77% after day 1 at around 100 ng/ml. • More sustained release of pBMP-9 over rhBMP-9. • LNP model of pBMP-9 delivery offers intravenous administration due to its low hemolytic potential.	[124, 126, 127, 147]
Collagen	Nano-hydroxyapatite (nHA)/collagen I (Col type I)/multi-walled carbon nanotube (MWCNT) composite scaffold loaded with rhBMP-9 nHA and MWCNT are nanofillers that facilitate scaffold mechanical properties along with enhancement of bioactivity.	• Interconnected porous three-dimensional structure for the scaffold; pore size reduced with an increase in MWCNT amount. • Increased MWCNT amount reduced water absorption and scaffold swelling but increased the mechanical strength of the scaffold. • Composite structure of the scaffold is a crucial parameter for tuning cellular interaction and subsequent bone regeneration.	• Adequate porosity with a uniform pore structure facilitates proper nutrient transport and reduces cell losses. • Osteoblast differentiation and subsequent new bone formation were enhanced with a BMP-9 loaded composite scaffold. • Enhanced cellular anchorage and cytoskeletal extension in the case of BMP-9 loaded composite scaffolds.	[129]
	Collagen Membrane	• Osteoblast behavior is enhanced by the collagen membrane; scaffold biomaterial has significantly more effect on cell attachment and proliferation over the use of BMPs.	• Osteopromotive potential increased by coupling porcine collagen membrane with BMP-9, in comparison to BMP-2. • A low dosage of BMP-9 (10 ng/ml) also displays promising osteogenic potential.	[141]
	nHA/Col/gelatin microsphere (GM) encapsulated with BMP-9. nHA acts as a nanofiller for enhanced bioactivity.	• Interconnected porous structure with nanofiller (nHA) deposition on a collagen matrix. • The freeze-drying technique is beneficial in rendering a porous structure to the scaffold. • Bone marrow mesenchymal stem cells (BMMSCs) displayed enhanced proliferation in the presence of scaffolds.	• Initial cell adhesion (3 h) was enhanced with the presence of scaffold, irrespective of the presence of BMP-9. • Scaffold porosity facilitated enhanced cell attachment; cells grew with an elongated morphology. • Porous scaffold provided adequate housing for the microsphere encapsulated BMP-9 with an effective release to activate BMMSCs.	[130]

Biomaterial(s) for Matrix	Delivery System/Model	Key Features	Advantages	References
		• Increased ALP activity in the scaffold groups from day 4. • No pathological changes along with any pyrogenic reactions were observed with the application of the porous scaffold.	• Biocompatible scaffold with adequate biodegradation with time.	
Methyl Cellulose and Alginate	Methylcellulose/ Alginate loaded with Chitosan microparticles coated with BMP-9.	• Methylcellulose is thermosensitive and becomes gel at close to physiological temperature. • VEGF was added to the gel scaffold to enhance angiogenesis. • The presence of BMP-9 in a normal medium in 2D culture displayed enhanced ALP activity.	• The blend of methylcellulose (with calcium chloride) with alginate provides adequate crosslinking and mechanical strength to the hydrogel scaffold. • Hydrogel scaffold facilitates a much more sustained release profile for microparticle coated BMP-9. • BMP-9 in an osteogenic medium enhances ALP activity the most; Alizarin red shows denser and more uniform biomineralization with BMP-9 loaded scaffold. • Injectable scaffold.	[139]
Biphasic calcium phosphate	Biphasic calcium phosphate (BCP) particles with BMP-9 adsorption	• Micro and macroporous surface of BCP particles. • Rough surface of BCP with observed nano topography.	• Adequate adsorption of BMP-9 on the biomaterial with sustained release up to day 10. • Enhanced osteogenic differentiation with rhBMP-9 loaded BCP scaffold, marked by PCR analysis and Alizarin red staining.	[140]
Fibrinogen and Thrombin	Fibrin Sealant (Brand Name: TISSEEL)	• Adequate housing for holding BMPs with a sustained release profile over days 10. • Local release of growth factors at the defect site or at the target for bone deposition.	• Fibrin sealant is biocompatible, biodegradable with low immunogenicity; safe for *in vivo* applications. • Enhanced osteogenic potential of fibrin sealant with the addition of rhBMP-9, as compared to using fibrin sealant alone.	[142]
Hyaluronic acid (HA)	HA crosslinked with butanediol diglycidyl ether.	• HA is an inert biocompatible material. • Crosslinked HA revealed a wavy structure with grooves and pits on its surface. • 70% of rhBMP-9 could be loaded on to the scaffold with a slow-release profile over 10 days.	• Cell growth in a three-dimensional scaffold with HA. • HA alone enhances osteocalcin expression on day 14; with the addition of rhBMP-9, the increase in osteogenic differentiation becomes two-fold. • Biomineralization, using alizarin red, display a similar trend that highlights the benefit of using HA.	[143]

Table 3.

Biomaterials in recent application for viral carrier mediated delivery of BMP-9.

Biomaterial (s) for Matrix	Delivery System/Model	Key Features	Advantages	References
Poly(polyethyleneglycol citrate-co-N-isopropylacrlamide) (PPCN) blended with Gelatin (PPCNG)	PPCNG scaffold with BMP-9 stimulated MSCs lineage progenitor immortalized cell lines (iMEFs or iCALs or iMADs) using adenoviral gene therapy.	• PPCN is a biocompatible and thermoresponsive polymer with a hierarchical structure of micropores and nanofibers. • PPCN can form a gel at 30 °C, which is adequate for gel formation at physiological temperature. • BMP-9 stimulated MSCs were distributed evenly in PPCNG. • Enhanced VEGF expression in PPCNG scaffold groups.	• PPCN gel retains original volume with gelation; negligible shrinkage. • Adequate biodegradation of PPCN at 4 to 5 weeks post-implantation. • The addition of gelatin enhances cell adhesion and survival. • The addition of gelatin in PPCN significantly improves transgene expression, reported through GLuc activity. • Cell interaction with scaffold enhances with gelatin addition to PPCN. • Uniformly distributed trabecular ectopic bone formation with a woven-like structure. • Neovascularization is enhanced with the addition of gelatin. • Injectable scaffold.	[152, 153] [154]
Gelatin-derived graphene and silicate nanosheets of Laponite (GL)	GL powder co-cultured with MSCs infected with adenoviral BMP-9.	• GL hybrid enhances the properties of gelatin. • A porous 3D structure that is stable to carbonization. • Laponite nanosheets are uniformly distributed in the carbon-rich matrix; mesopores in the carbon-rich bulk matrix was observed.	• Complexation with GL hybrid enhances the thermal stability of gelatin. • Adequate pore size facilitates cellular distribution within the scaffold. • Cells populated on inner and outer surfaces of the scaffold; the scaffold is osteoconductive. • Trabecular ectopic bone structure formation with BMP-9 transduced iMEFs. • The synthesis of the GL scaffold is inexpensive and easily scalable.	[155]
Coralline hydroxyapatite (CHA)	CHA loaded with AdBMP-9 transfected rat dental follicle stem cells (rDFCs).	• CHA is a biocompatible and conductive material. • Highly porous CHA scaffolds with a maximum pore size of 600 μm; interconnected pore structure. • Vascularization along with fibrous tissue formation was observed with rDFC/CHA scaffold group with BMP-9.	• Cell attachment and proliferation enhanced with the porous structure of the scaffold; complete coverage with cells on day 7. • ALP, OPN, and Osx expression levels enhanced with CHA during co-culture of rDFCs even in a normal medium; osteogenic medium results may be hypothesized to be higher.	[156]

Mater Sci Eng C Mater Biol Appl. Author manuscript; available in PMC 2022 January 01.

Biomaterial (s) for Matrix	Delivery System/Model	Key Features	Advantages	References
		• New bone formation was observed around the CHA scaffold area with BMP-9 loaded scaffold groups.		